

# Response to Referee #1

*General Comments:* This paper introduces a method to access the wet removal rate of BC in East Asia based on long-term measurements, in the aspect of the air mass back trajectories. The authorship made effort to obtain the overall wet removal rates of BC as a function of accumulated precipitation along trajectories, the half-life and  $e$ -folding lifetime. Depending on the measurement sites, the wet removal rates of BC showed large regional differences, and various reasons are explored. Further, they diagnosed the scavenging coefficients of the below- and in-cloud scavenging scheme implemented in the FLEXible PARTicle (FLEXPART) Lagrangian transport model with the obtained wet removal rates of BC, and suggested that underestimation of wet scavenging coefficients in the model simulation. Finally, they evaluated the relative importance of various factors in the in-cloud scavenging process, and indicated that the convective available potential energy should be considered to better represent the regional difference of BC wet scavenging over East Asia. The topic of the manuscript is well suited for publication in ACP. The long-term dataset are generally applicable, whereas some discussions are lack of persuasion. I suggest more effort should be put into the presentation of the results before publication. My major concern is about the preset for the calculation and the reasons for the regional difference of wet removal efficiency.

Response: We thank the reviewer for carefully reviewing the manuscript and providing valuable comments. We also acknowledge your valuable comments and suggestions that greatly helped to improve the manuscript. The following are our responses to your specific comments. For convenience, your comments are italicized and numbered. The line (L) numbers in the responses correspond to those in the revised manuscript. The changes in the revised manuscript are underlined in the responses as necessary, and are indicated as ‘tracked changes’ in the manuscript.

1. *The authors used 500 m as a starting altitude and 72h back trajectories were calculated. Is it an arbitrary selection? How does this affect the final assessment of wet removal?*

We replaced the past 72 h backward trajectory, which can represent the wet deposition effects, to the past 120 h by considering the BC lifetime ( $\sim 5$  d) and including dry deposition effects; however, the results are exactly the same as in the original manuscript because identified potential emission source regions are consistent with the original manuscript. The difference in the starting altitude (500 m vs. 1000 m) did not impact our results; i.e., the ranges of the TE for sites, regions and seasons used in Table 1 and below- and in-cloud cases in Table 2 were similar to the original results (Sect. S1 in the Supplement). A detailed explanation of the uncertainty due to the selection of different starting altitudes was addressed as follows:

“To identify the air mass origin region, 5 d (72 120 h) backward trajectories were calculated four times a day (00, 06, 12, 18 UTC) using the Hybrid Single Particle Lagrangian Integrated Trajectory (HYSPLIT) Model version 4 (Draxler et al., 2018). The starting altitude was 500 m above ground level (AGL). The past 120 h of backward simulation time was selected by considering the lifetime of BC ( $\sim 5$  d; Lund et al., 2017, 2018; Park et al., 2005). It should be noted that the different starting altitude (500 m vs. 1000m) did not impact on our results (Sect. S1 in the Supplement).” (L140–144)

“Our main results, including the TE,  $\Lambda_{\text{below}}$ , and  $\Lambda_{\text{in}}$ , could be influenced by selecting (1) different starting altitudes of the backward trajectories and (2) different altitude criteria for identifying the potential emission region.

First, to investigate the uncertainty caused by different starting altitudes of the backward trajectories, we analyzed the Welch’s  $t$ -test for APT derived from starting altitudes of 500 m and 1000 m. The APT between the two datasets did not show a significant difference (3%) ( $p \geq 0.1$ ). Depending on the site, the TE showed a significant difference ( $p < 0.05$ ) at Gosan only at a relatively small value of  $-4.2\%$ . In the case of regional TE, Northeast China and South Korea were significantly different ( $p < 0.01$ ), with original values up to  $-15\%$ ; however, the corresponding APT for achieving TE=0.5 and TE=1/e

only decreased by  $-6\%$  and  $-2\%$ , respectively. The regional wet removal efficiency was more apparent, such as more or less APT needed to attain  $TE=0.5$  and  $TE=1/e$  in low-efficiency regions (East and North China) and high-efficiency regions (South Korea and Japan), respectively. For the high starting altitude, i.e., 1000 m, the airmass had a higher chance of being exposed to in-cloud scavenging resulting in a much lower TE for in-cloud scavenging ( $-3\%$ ). Otherwise, the TE for below-cloud scavenging cases was increased by  $7\%$  because of a reduced chance to expose washout effects (Table S1). Because of the variations in the TE for below- and in-cloud scavenging cases, the calculated median  $\Lambda_{\text{below}}$  and  $\Lambda_{\text{in}}$  converged within a similar range as the original results. It should be noted that the median measured  $\Lambda_{\text{below}}$  was slightly higher than the calculated  $\Lambda_{\text{below}}$  according to FLEXPART, which is opposite the original results. The small difference could be ignored when considering the insufficient sample number for below-cloud cases at a starting altitude of 1000 m.” (Sect. S1 in the Supplement)

**Table S1.** Same as Table 2 except for the different backward trajectory starting altitudes (1000 m)

Cases	Median	Interquartile range (25 <sup>th</sup> percentile – 75 <sup>th</sup> percentile)
(a) Below cloud ( $N_{\text{case}} = 262$ )		
TE	0.95	[0.65 – 1.28]
Measured $\Lambda_{\text{below}}$ ( $\text{s}^{-1}$ )	$8.85 \times 10^{-6}$	$[6.57 \times 10^{-6} - 1.46 \times 10^{-5}]$
Calculated $\Lambda_{\text{below}}$ ( $\text{s}^{-1}$ ) <sup>a</sup>	$7.49 \times 10^{-6}$	$[6.83 \times 10^{-6} - 8.42 \times 10^{-6}]$
(b) In-cloud ( $N_{\text{case}} = 953$ )		
TE	0.70	[0.46 – 1.02]
Measured $\Lambda_{\text{in}}^*$ ( $\text{s}^{-1}$ ) <sup>b</sup>	$7.67 \times 10^{-5}$	-
Calculated $\Lambda_{\text{in}}^*$ ( $\text{s}^{-1}$ ) <sup>a,b</sup>	$8.01 \times 10^{-6}$	-

<sup>a)</sup> Calculated by FLEXPART scheme

<sup>b)</sup> Overall median value

2. *The authors attributed the regional difference in wet removal efficiency to the difference in the coating thickness of BC particles. In the discussion section, they consider that depending on the emission sectors, the coating thickness of BC particles could be a major factor causing the difference in the wet removal efficiency. I think such explanation is hard to believe. The freshly emitted BC particles has transported for a long distant before scavenged. How could the freshly emitted BC particles affect their coating thickness before scavenged? Actually, there are many published paper showing factors that drive the ageing of BC, which should be included in the discussion.*

We agree with the reviewer’s opinion that the BC aging process is most important when considering the predominance of in-cloud scavenging. Therefore, we added the description of the BC aging process and frequency of below- and in-cloud scavenging conditions as the most plausible reasons causing regional and seasonal differences in wet scavenging efficiency. The explanation of difference in coating thickness of BC upon emission was removed because of the lack of evidence supporting our hypothesis.

“According to the relationship between accumulated precipitation along trajectory and TE, ~~TE~~ the wet removal efficiency was lower in East and North China, where the industrial sector (thin coated) is dominant; in contrast, that but higher in South Korea and Japan showed higher values, implying the importance of the aging process and frequency of exposure to below- and in-cloud scavenging conditions during airmass transport ~~due to the transport sector (thick coated), with emissions mainly from diesel vehicles. By the same token~~ Moreover, ~~TE~~ the wet scavenging in winter and summer showed the highest and lowest values efficiency, respectively, although the lowest removal efficiency in summer was primarily associated with a reduced BC aging process because the in-cloud scavenging condition was dominant, depending on the dominant emission sectors, such as house heating (thick-coated) and industry.”(L23–30)

“According to the pathway of airmass transportation, the detailed meteorological information ~~for~~, such as precipitation (sum of large-scale and convective precipitation), ~~and clouds, and so on,~~ was

acquired based on the air mass transportation pathway from ERA5 hourly data at both single and pressure levels (37 levels; 1000 hPa to 1 hPa) to identify the below- and/or in-cloud cases and to calculate the wet scavenging coefficients. By considering the vertical height of the air mass from the HYSPLIT model and cloud information from ERA5, we successfully distinguished the dominant cases for below-cloud (no residence time within cloud) and in-cloud (no residence time below cloud) cases when precipitation  $\geq 0.01 \text{ mm hr}^{-1}$  and calculated the wet scavenging coefficients.” (L148–153)

“The differences in regional and seasonal wet removal rates could be explained might be influenced by the frequency of exposure to below- and in-cloud scavenging condition during transport as well as the magnitude of aging process causing the different coating thicknesses the different coating thicknesses according to the BC emission sources (thin and thick coated BC from the industrial and residential sectors, respectively) because the thick-coated BC particles are preferentially removed due to cloud processes.” (L461–465)

“To quantify the effect of below- and in-cloud scavenging, we investigated the fraction of exposure to below- and in-cloud scavenging conditions during the air mass transport according to regions. Among the total frequency of grid cells which air mass passed (~500,000), ~25% of the grid cells were exposed to below- (~10%) and in-cloud scavenging conditions (~15%), indicating that the in-cloud conditions were relatively predominant in wet scavenging over East Asia. The higher wet removal efficiency region (South Korea and Japan) revealed an apparently higher fraction of exposure to below- (~11%) and in-cloud scavenging conditions (~19%) compared to the air mass from East and North China (~8% for below- and ~10% for in-cloud scavenging condition), suggesting the importance of in-cloud scavenging process for wet deposition.

Second, the difference in the degree of BC aging process could be an important factor for determining the wet scavenging efficiency. Freshly emitted BC particle have small diameters, exhibit a thin coating thickness, and are hydrophobic; thus, they would not be effective in wet scavenging compared to aged BC particles. Typically, the coefficient of BC aging rate in North China Plain was significantly higher than that used in previous models (e.g., Cooke and Wilson, 1996; Koch and Hansen, 2005; Xu et al., 2019) due to the highly polluted environments (Zhang et al., 2019); however, the coefficients over East Asia are still unknown. In addition, the median regional traveling time of air masses to each site (11–47 h for Baengnyeong; 18–37 h for Gosan; 19–62 h for Noto) was different. Therefore, the difference in both the level of BC aging coefficient and traveling time depending on the region, which can influence the coating thickness of BC particles, might be another plausible reason underlying the regional differences in the wet removal efficiency the difference in the coating thickness of BC particles, depending on the emission sectors, could be a major factor causing the difference in the wet removal efficiency because thickly-coated BC particles are much easier to remove by wet scavenging than less coated and/or freshly emitted BC (Ding et al., 2019; Miyakawa et al., 2017; Moteki et al., 2012). Typically, BC emitted from industrial regions, transport from diesel vehicles, and domestic sectors has characteristics of weakly, moderate, and strongly coated BC, respectively (Han et al., 2019; Liu et al., 2019), based on insignificant differences in the MMD of BC from those emission sectors (190–200 nm). This result coincided with the major emission sector of the REAS emission inventory in East and North China and North Korea (~57.5% emitted from industrial sectors) compared to other sites (12%–39%). In contrast, Northeast China showed low APT for reaching  $TE=0.5$  and  $TE=1/e$  because the dominant BC emission sector was residential sector (48.3%) which has a thickly coated characteristic. BC from South Korea and Japan reached  $TE=0.5$  and  $TE=1/e$  with a small amount of APT because moderately coated BC was mostly emitted from the transport sector (73.4%), mainly from diesel vehicles. It should be noted that the dominant emission sectors of industry (for East and North China and North Korea) or transport sectors (South Korea and Japan) were also confirmed by the Emission Database for Global Atmospheric Research (EDGAR) in 2010 and MIX in 2010 (Li et al., 2017; Crippa et al., 2018).

By the same token, in the case of seasonal variation in  $TE$  wet removal efficiency, the decreasing

magnitude of TE according to APT was obviously emphasized in fall and winter, which was much steeper than that in spring and summer (Figure 4b). This tendency was reflected differences in not only the degree of aging process, but also the fraction of exposure to below- and in-cloud scavenging conditions. The fraction of below- and in-cloud scavenging in spring were lower at ~7% and ~11%, respectively, compared to those in fall and winter (11% for below- and 16% for in-cloud scavenging conditions). The fraction of in-cloud scavenging cases was the highest in summer (17%) compared to the other seasons, but the APT for reaching TE=0.5 was also high, indicating that the removal efficiency of in-cloud scavenging was reduced. Considering the less pollution in summer, the lowest wet removal efficiency might be fully explained by the low coefficient of BC aging rate compared to that in other seasons (Zhang et al., 2019) in the effect of the residential sector, which has thickly coated BC, which increased due to house heating as the temperature decreased. In contrast to winter, the APT for reaching TE=0.5 in spring and summer was the highest among the seasons. This might be caused by the increasing fraction of BC from the industrial sector in China while decreasing emissions from residential sectors (Kurokawa et al., 2013)." (L274–315)

*Specific comments:*

1. *Introduction: "Specifically, the in-cloud process is more efficient and complicated than the below-cloud process because the nucleation removal of aerosol particles within clouds is thought to account for more than 50% of the aerosol particle mass removal from the atmosphere globally" I wonder if there are any scavenging efficiency data for BC alone, since this paper mainly focus on the wet removal of BC.*

We replaced the sentences to focus on BC particles as follows:

"Wet deposition of BC, whose contribution to total removal is 79% (Textor et al., 2006), is still challenging to predict BC concentrations in the atmosphere due to the difficulties of accurate evaluation of wet removal (Emerson et al., 2018; Bond et al., 2013; Lee et al., 2013). Specifically, the in-cloud process is more efficient and complicated than the below-cloud process because the nucleation removal of aerosol particles within clouds is thought to account for ~~more than 50~~  $46 \pm 50\%$  of the ~~aerosol~~ BC particle mass removal from the atmosphere globally, although this is dependent on the selected global model (Grythe et al., 2017; Textor et al., 2006)." (L61–66)

2. *Introduction: "Wet deposition is still challenging to predict BC concentration in the atmosphere due to the difficulties of accurate evaluation of wet removal." It would be better to include more explanation on why it is challenging to represent wet deposition, which tightly links to the discussion section of this paper.*

We added a detailed description of the reasons for the difficulties in accurately evaluating the wet removal of BC as follows:

"This can partly be attributed to the following three reasons: (1) inaccurate bottom-up emission inventory, (2) the complexity of BC hygroscopicity, and (3) an imprecise dry/wet deposition scheme. First, when estimating the impact of BC using global models, the results usually contain large uncertainties in BC emissions (Cooke and Wilson, 1996; Chung and Seinfeld, 2002; Stier et al., 2007) because BC is mainly contributed by scattered emission sources. Therefore, the uncertainty of BC emission rates is large compared to other species (e.g., SO<sub>2</sub>, NO<sub>x</sub>, and CO<sub>2</sub>) whose emissions are dominated by large sources (Kurokawa et al., 2013; Zheng et al., 2018). Without appropriate constraints on the emissions, removal cannot be well quantified. Second, although BC itself is hydrophobic immediately after emission, it is subsequently converted to possessing hydrophilic properties through the aging process, in which water-soluble compounds coat BC, and during atmospheric transportation (Moteki et al., 2007; Matsui et al., 2018), and finally acts as cloud condensation nuclei (Kuwata et al., 2007; Bond et al., 2013). Such conversion depends on the initial state of the BC along with atmospheric conditions (presence of other particles and gases) and it has high spatial and temporal variabilities (Vignati et al., 2010)." (L49–59)

“However, there is insufficient in-field detailed observations to explain and quantify the interactions between BC and cloud particles at the microscale, which hinders a better understanding of the physical processes (Ding et al., 2019).” (L66–68)

3. *Introduction: It would be better to simply explain “emission rates and deposition terms”.*

We provided additional detail regarding the ‘emission rates and deposition terms’ as follows:

“Although some previous studies have investigated wet scavenging schemes in models (Grythe et al., 2017; Croft et al., 2010), those results without well-constrained emission rates contain large ambiguity when assessing the wet deposition term (Vignati et al., 2010) may include bias due to the effect of inaccurate emission rate because emission rates and deposition terms were not necessarily separated. For the first time, the emission and deposition terms are distinctly separated in this study by introducing TE and using backward simulations,; this allows thus allowing for the wet scavenging scheme to be evaluated more accurately because backward simulations do not account for the emission rate.” (L92–98)

4. *Experimental section: “when the air mass altitude was lower than 2.5 km...”. Is there any explanation for this?*

We added a discussion of the uncertainty in the criteria for selecting the altitude as follows:

“We checked the uncertainty arising from selecting different criteria for altitude (1.5 km), but there was no significant difference in the results (Sect. S1 in the Supplement).” (L171–172)

“Second, we also checked the difference in wet scavenging efficiency, which can be caused by applying 1.5 km (instead of 2.5 km) as a threshold to determine the potential emission region. The identified six administrative districts for potential emission regions at an altitude of 1.5 km were same as those at an altitude of 2.5 km. The median traveling time from potential source regions to receptor sites was decreased from 38 h to 25 h when precipitation occurred because the individual potential source region was closer to the receptor site because the selection altitude was decreased. However, the difference in traveling time did not significantly influence our final results because the TE for below- and in-cloud cases only decreased by 1% and 6% and the measured  $\Lambda_{\text{below}}$  and  $\Lambda_{\text{in}}$  were consistent with the original results within  $\pm 54\%$  (Table S2). From these results, we confirmed the representativeness of our regional and seasonal wet removal efficiency analysis.” (Sect. S1 in the Supplement)

**Table S2.** Same as Table 2 except for the different altitude criteria (1.5 km) for identifying potential emission source regions.

Cases	Median	Interquartile range (25 <sup>th</sup> percentile – 75 <sup>th</sup> percentile)
(a) Below cloud ( $N_{\text{case}}=436$ )		
TE	0.88	[0.60 – 1.24]
Measured $\Lambda_{\text{below}}$ ( $\text{s}^{-1}$ )	$6.17 \times 10^{-6}$	$[2.55 \times 10^{-6} - 1.39 \times 10^{-5}]$
Calculated $\Lambda_{\text{below}}$ ( $\text{s}^{-1}$ ) <sup>a</sup>	$7.52 \times 10^{-6}$	$[6.88 \times 10^{-6} - 8.50 \times 10^{-6}]$
(b) In-cloud ( $N_{\text{case}}=282$ )		
TE	0.68	[0.44 – 1.03]
Measured $\Lambda_{\text{in}}^*$ ( $\text{s}^{-1}$ ) <sup>b</sup>	$9.39 \times 10^{-5}$	-
Calculated $\Lambda_{\text{in}}^*$ ( $\text{s}^{-1}$ ) <sup>a,b</sup>	$8.15 \times 10^{-6}$	-

<sup>a)</sup> Calculated by FLEXPART scheme

<sup>b)</sup> Overall median value

5. *Line 199-: Is there any correlation between wet removal of BC and meteorological parameters?*

The median TE as a function of the site showed a good correlation with the precipitation rate and total column cloud water ( $R \geq 0.94$ ) and moderate correlation with cloud cover and cloud bottom heights ( $R \geq 0.52$ ) because only three data records were available. Thus, we did not add the R value between two variables in this qualitative analysis section because a detailed analysis was conducted in the

following sections according to the back trajectories along with their meteorological conditions.

Minor:

1. *Line 65: “stat”?*

We revised it to ‘states.’ (L81)

2. *Line 73: “significant”?*

We changed this term to ‘considerable.’

“Recently, numerous fine mode particles, including BC<sub>1</sub> from polluted areas scavenging in clouds were more pronounced in East Asia, not only at a local scale but also at a large regional scale (Liu et al., 2018), because high aerosol loading conditions are usually associated with considerable significant cloud cover, which results in a higher frequency of wet scavenging (Eck et al., 2018).” (L84–87)

3. *Line 136: “good spatial coverage”?*

We replaced ‘good spatial coverage’ with a detailed description.

“Figure 1c reveals the geographical distribution for the mean BC mass of identified potential emission regions, indicating that this approach was appropriate because ~~of good spatial coverage~~ the potential emission regions were uniformly distributed over East Asia, including East China, a major emission source for BC.” (L167–169)

4. *Line 149: “thus the TE was an effective indicator”.*

We revised it as follows:

“... thus the TE ~~was~~ is an effective indicator ...” (L184)

5. *Line 193: “However”?*

We deleted the conjunction ‘however’.

~~“However, previous~~ Previous studies reported that the mass median diameter (MMD) ...” (L236)

## Response to Reviewer #2

### General comments:

*The paper addresses a topic of scientific relevance which is within the scope of Atmospheric Chemistry and Physics. They present a method to evaluate the wet removal rate of black carbon (BC) with the LPDM Flexpart based on long-term measurements over East Asia. The authors used back-trajectories with Hysplit to identify the source region of the air masses from 3 stations over East Asia and to determine the accumulated precipitation along the trajectories. With this information, they calculated the Transport Efficiency (TE) of black carbon from the measurements and compared the TE from measurements with the results of the backward modelling with Flexpart v10.4 to assess the simulated wet removal rate in transport modelling. Additionally, the authors further distinguish their evaluation between below cloud and in-cloud wet removal by diagnosing the scavenging coefficients. They show that the wet removal of BC from the different measurement sites have significant differences and discuss various reasons. According to the scavenging from below and in-cloud, they found that Flexpart underestimates the in-cloud scavenging and overestimates the below-cloud scavenging. By using a neural network, the authors investigated the importance of several dependencies. They found that CAPE is the parameter with the most substantial influence on in-cloud scavenging and suggest to include this parameter in the future.*

Response: We thank the reviewer for carefully reviewing the manuscript and providing valuable comments. We also acknowledge your valuable comments and suggestions that greatly helped to improve the manuscript. The following are our responses to your specific comments. For convenience, your comments are italicized and numbered. The line (L) numbers in the responses correspond to those in the revised manuscript. The changes in the revised manuscript are underlined in the responses as necessary and indicated using ‘tracked changes’ in the manuscript.

*However, even though the methods and discussions provide valuable assets to the community, they are not easy to understand and clear in the way it was written. I had to re-read multiple sections to identify what was done and which values from which data sets were compared or used. In my opinion, this could be improved by some additional definitions and distinctions. For example, the authors should clearly distinguish between measured data, determined/calculated data and simulated data. For example, I often got confused by the mentioning of Flexpart scheme, since this was sometimes the simulated data and sometimes the algorithm for deposition calculation. I suggest major revisions as outlined in the comments below and addressing the specific comments before publishing the manuscript.*

We tried to clarify the terminology through the entire manuscript. Only the measured TE was compared with the simulated TE from FLEXPART, and the measured below- and in-cloud scavenging coefficients were compared with those calculated according to the FLEXPART scheme. Therefore, we used different terminology when addressing the FLEXPART value: 'simulated' for the output from FLEXPART and 'calculated' for following the FLEXPART scheme. In light of the comments, we have now unified the terminology from ‘estimated’ to ‘measured’ when discussing the outputs derived from the measured TE. To prevent misunderstanding, we added the following statements:

“Note that the simulated TE from FLEXPART (FLEXPART TE) was only used for comparing with the measured TE.” (L206–207)

“From this section, we aimed to investigate the below- and in-cloud scavenging in detail by discriminating the representative cases according to cloud information from the ERA5 pressure level data with HYSPLIT backward trajectory to overcome the limitation of the local variability of meteorological input variables.” (L344–346)

“..., we compared our measured scavenging coefficients with those calculated according to FLEXPART scheme (not simulated).” (L349–350)

“It should be mentioned that  $\Lambda_{in}$  was also calculated by following the FLEXPART scheme using the ERA5 meteorological data ( $0.25^\circ \times 0.25^\circ$ ) with HYSPLIT backward trajectory instead of the FLEXPART simulation ( $1^\circ \times 1^\circ$ ) to reflect the local variability of meteorological variables ~~match the grid size of the input data with the HYSPLIT backward trajectory.~~” (L400–402)

“The FLEXPART calculated  $\Lambda_{in}^*$  ( $7.28 \times 10^{-6} \text{ s}^{-1}$ ) from FLEXPART scheme (hereafter calculated  $\Lambda_{in}^*$ ) was underestimated by 1 order of magnitude compared to our ~~estimated~~ measured  $\Lambda_{in}^*$  ( $8.06 \times 10^{-5} \text{ s}^{-1}$ ).” (L406–407)

#### Major comments:

1. *How did you select the simulation setup? Why only 72h of backward runs and why starting with a height of 500m for the release location? There must have be some investigation or thought on this. What effect does it have on the results?*

We replaced the past 72 h backward trajectory, which can represent the wet deposition effects, to the past 120 h by considering the BC lifetime ( $\sim 5$  d) and including dry deposition effects; however, the results are exactly the same as in the original manuscript because identified potential emission source regions are consistent with the original manuscript. The difference in the starting altitude (500 m vs. 1000 m) did not impact our results; i.e., the ranges of the TE for sites, regions and seasons used in Table 1 and below- and in-cloud cases in Table 2 were similar to the original results (Sect. S1 in the Supplement). A detailed explanation of the uncertainty due to the selection of different starting altitudes was addressed as follows:

“To identify the air mass origin region, 5 d (72 120 h) backward trajectories were calculated four times a day (00, 06, 12, 18 UTC) using the Hybrid Single Particle Lagrangian Integrated Trajectory (HYSPLIT) Model version 4 (Draxler et al., 2018). The starting altitude was 500 m above ground level (AGL). The past 120 h of backward simulation time was selected by considering the lifetime of BC ( $\sim 5$  d; Lund et al., 2017, 2018; Park et al., 2005). It should be noted that the different starting altitude (500 m vs. 1000m) did not impact on our results (Sect. S1 in the Supplement).” (L140–144)

“Our main results, including the TE,  $\Lambda_{below}$ , and  $\Lambda_{in}$ , could be influenced by selecting (1) different starting altitudes of the backward trajectories and (2) different altitude criteria for identifying the potential emission region.

First, to investigate the uncertainty caused by different starting altitudes of the backward trajectories, we analyzed the Welch’s *t*-test for APT derived from starting altitudes of 500 m and 1000 m. The APT between the two datasets did not show a significant difference (3%) ( $p \geq 0.1$ ). Depending on the site, the TE showed a significant difference ( $p < 0.05$ ) at Gosan only at a relatively small value of  $-4.2\%$ . In the case of regional TE, Northeast China and South Korea were significantly different ( $p < 0.01$ ), with original values up to  $-15\%$ ; however, the corresponding APT for achieving TE=0.5 and TE=1/e only decreased by  $-6\%$  and  $-2\%$ , respectively. The regional wet removal efficiency was more apparent, such as more or less APT needed to attain TE=0.5 and TE=1/e in low-efficiency regions (East and North China) and high-efficiency regions (South Korea and Japan), respectively. For the high starting altitude, i.e., 1000 m, the air mass had a higher chance of being exposed to in-cloud scavenging resulting in a much lower TE for in-cloud scavenging ( $-3\%$ ). Otherwise, the TE for below-cloud scavenging cases was increased by  $7\%$  because of a reduced chance to expose washout effects (Table S1). Because of the variations in the TE for below- and in-cloud scavenging cases, the calculated median  $\Lambda_{below}$  and  $\Lambda_{in}$  converged within a similar range as the original results. It should be noted that the median measured  $\Lambda_{below}$  was slightly higher than the calculated  $\Lambda_{below}$  according to FLEXPART, which is opposite the original results. The small difference could be ignored when considering the insufficient sample number for below-cloud cases at a starting altitude of 1000 m.” (Sect. S1 in the Supplement)



**Table S2.** Same as Table 2 except for the different backward trajectory starting altitudes (1000 m)

Cases	Median	Interquartile range (25 <sup>th</sup> percentile – 75 <sup>th</sup> percentile)
(a) Below cloud ( $N_{case} = 262$ )		
TE	0.95	[0.65 – 1.28]
Measured $\Lambda_{below}$ ( $s^{-1}$ )	$8.85 \times 10^{-6}$	$[6.57 \times 10^{-6} - 1.46 \times 10^{-5}]$
Calculated $\Lambda_{below}$ ( $s^{-1}$ ) <sup>a</sup>	$7.49 \times 10^{-6}$	$[6.83 \times 10^{-6} - 8.42 \times 10^{-6}]$
(b) In-cloud ( $N_{case} = 953$ )		
TE	0.70	[0.46 – 1.02]
Measured $\Lambda_{in}^*$ ( $s^{-1}$ ) <sup>b</sup>	$7.67 \times 10^{-5}$	-
Calculated $\Lambda_{in}^*$ ( $s^{-1}$ ) <sup>a,b</sup>	$8.01 \times 10^{-6}$	-

<sup>a)</sup> Calculated by the FLEXPART scheme

<sup>b)</sup> Overall median value

2. *Why do you use two different models with a different data set each? This causes a lot of differences and uncertainties in the results. You mention that you did not find large differences in the pathways between Hysplit with ERA5 and Flexpart with ERA Interim. But there are still differences due to the different physical parameterizations and spatial and temporal resolutions. Wouldn't it be more accurate to use Flexpart for the trajectory calculations also and therefore use the same data set? I know that ERA5 model level data were not easily available for all users in the past, but it is now. Therefore, it would be a substantial improvement to use the same data set, namely ERA5, for all simulations. I am aware that this is probably not possible to achieve within this review process, but the authors should discuss this and provide more details about possible uncertainties.*

We agree with the reviewer's opinion that the consistency of the FLEXPART simulation with ERA5 could be strengthened to demonstrate the robustness of our results compared with the use of only the results from the HYSPLIT model. However, we do not have authorization to access ERA5 through 'flex\_extract' because we are a 'public user' who can access the ERA-Interim. However, the ERA5 for HYSPLIT model is open access.

Although we used different meteorological fields (ERA5 for HYSPLIT and ERA-Interim for FLEXPART), the calculated below- and in-cloud scavenging coefficients were derived using HYSPLIT model with ERA5 vertical meteorological information according to the FLEXPART scheme. Only the TE were compared and verified with that from FLEXPART with ERA-Interim. Although the detailed meteorological parameters were different according to their temporal (1 h vs. 6 h) and spatial ( $0.25^\circ$  vs.  $1^\circ$ ) resolutions, Hoffmann et al. (2019) reported that the particle positions (latitude, longitude, and altitude) along a 10-day forward trajectory calculated with both ERA-Interim and ERA5 showed good agreement. We also demonstrated an insignificant difference in air mass pathways between HYSPLIT and FLEXPART, and the following was added to the manuscript:

“Despite the difference in the input meteorological fields between HYSPLIT and FLEXPART, the difference in air mass pathways and APT between two datasets can be neglected (Hoffmann et al., 2019; Sect. S2 in the Supplement).” (L207–L209)

“We investigated the uncertainty in the air mass pathway and APT between HYSPLIT model using ERA5 and FLEXPART using ERA-Interim during study periods at three sites. It should be noted that the trajectory of FLEXPART was selected as the center of the main grid ( $1^\circ \times 1^\circ$ ) according to the highest residence time in the same time interval and then compared with HYSPLIT results by calculating the distance between two hourly endpoints. Thus, differences of less than  $\sim 100$  km can be regarded as a good agreement when considering the grid resolution of FLEXPART. The difference in distance increased as the traveling time was increased. However, the median traveling time of air masses, including APT=0 case, was 31 h, which showed a difference in distance of  $\sim 100$  km. When the traveling time was expanded up to the 75<sup>th</sup>ile of the traveling time (50 h), the difference in distance was close to  $\sim 200$  km. Although the difference in distance at 72 h traveling

time was high, 72 h traveling time cases was so rare that we could neglect the impacts on our results. In total, the median difference in distance was ~47 km, suggesting good agreement between the two datasets. In addition, the difference in accumulated backward-trajectory endpoints was much smaller because random errors in the single calculations can be diminished by increasing the number of calculations (Gebhart et al., 2005; Jeong et al., 2017).” (Sect. S2 in the Supplement)

3. *It is not recommended to use all four analysis times (0,6,12 and 18 UTC) per day and combine them with forecast fields to achieve 3-hourly temporal resolution. This causes unnecessary inconsistencies between 5h and 7h as well as 17h and 19h. The recommendation is to use 0 and 12 UTC and fill the times in between with forecast fields. I also thought that ERA-Interim on model levels were only available at 0,6,12 and 18UTC for public users, which gives me the indication that the access method was as a member-state user? Is this correct? Then you should have had access to ERA5 data all the time anyway.*

Thank you for correcting the information for ERA-Interim. We used the 0 and 12 UTC analysis times and filled the times in between with forecast fields as meteorological input data for FLEXPART.

“Temporally, ECMWF ERA-Interim has a resolution of 3 h, with ~~6~~ 12 h analysis and 3 h forecast time steps.” (L196–197)

Despite not being a member-state user, we modified the ‘flex\_extract’ code to access the ERA-Interim data, which has a 3-hourly resolution with an analysis and forecast field mix in the full-access mode.

4. *After going through the manuscript I had a hard time to distinguish which data set and scheme/formula was used to calculate TE or scavenging coefficients. I would highly suggest to go through section 3.4 and 3.5 (below and in-cloud scavenging) again and try to be more clear in the description and distinguishing of where a scavenging coefficient comes from. Maybe by giving it different subscriptions.*

Please refer to the main response. We tried to improve the readability by unifying (replacing ‘estimated’ with ‘measured’) or differentiating (‘simulated’ and ‘calculated’) the terminology throughout the manuscript.

#### Specific comments:

1. *p.1 l.29: You mention diagnosing the scavenging coefficients from Flexpart. I thought that Flexpart defines the coefficients upfront in a species file. Therefore, I don’t understand why the coefficients need to be diagnosed. Could you explain please?*

As you may already know, the species file (#40 for BC) contains the parameters for various efficiencies, such as the below-cloud collection efficiency for rain (pcrain\_aero) and snow (pcsnow\_aero) and in-cloud nuclei efficiency for cloud condensation (pccn\_aero) and ice (pin\_aero). The scavenging coefficients for in- and below-cloud are not included in the species file but are embedded in FLEXPART. Therefore, the purpose of our study, i.e., ‘diagnosing the scavenging coefficients of FLEXPART’, is necessary for evaluating BC accurately.

2. *p.2 l. 58: . . . because TE has been proven . . . ; could you provide evidence*

We added a reason for the statement as follows:

“Accompanied with the refinement of BC emission inventories over East Asia (Choi et al., 2020; Kanaya et al., 2016), wet removal rates have been ~~one of the main topics~~ a focal point to better predict BC behavior by using the term transport efficiency (TE), which is the observationally-determined fraction of undeposited BC particles during transport (e.g., Oshima et al., 2012; Kondo et al 2016), because TE shows a good relationship with accumulated precipitation along trajectory

(APT; sum of precipitation over the past 72 h backward trajectory) (Choi et al., 2020; Kanaya et al., 2016) TE has been proven to be a good proxy for wet scavenging.” (L69–74)

3. p.2 l. 65: *what is meant by “mixing stats”?*

We apologize for the mistake; we intended to write ‘mixing states,’ which has been corrected.

“... the BC size distribution and mixing states during the spring of 2015 at the same location.” (L81)

4. p2. l.68-71: *This sentence is hard to understand, especially the part with “...polluted areas scavenging in cloud were more...”.*

The statement means that the pollution from East Asia might be more exposed to below- and/or in-cloud scavenging because high aerosol loading conditions are usually associated with significant cloud cover in East Asia. We added the following:

“... because high aerosol loading conditions are usually associated with ~~significant~~ considerable cloud cover, which results in a higher frequency of wet scavenging (Eck et al., 2018).” (L85–87)

5. p.2 l.73: *... could be a useful parameter . . . ; I thought it is a useful parameter, why could?*

We revised this as follows:

“BC and carbon monoxide (CO) are byproducts of the incomplete combustion of carbon-based fuels, and the ratio between  $\Delta BC$  (the difference from the baseline level) and  $\Delta CO$  ~~could be~~ is a useful parameter for characterizing ~~combustion fuel types. due to~~ because of their different carbon contents (Zhou et al., 2009; Guo et al., 2017).” (L88–90)

6. p.2 l.74: *You mention that you adopt APT. You adopt it from where and how?*

We added a description of APT as follows:

“Accompanied with the refinement of BC emission inventories over East Asia (Choi et al., 2020; Kanaya et al., 2016), wet removal rates have been ~~one of the main topics~~ a focal point to better predict BC behavior by using the term transport efficiency (TE), which is the observationally-determined fraction of undeposited BC particles during transport (e.g., Oshima et al., 2012; Kondo et al 2016), because TE shows a good relationship with accumulated precipitation along trajectory (APT; sum of precipitation over the past 72 h backward trajectory) (Choi et al., 2020; Kanaya et al., 2016) TE has been proven to be a good proxy for wet scavenging.” (L69–74)

7. p.3 l.82: *What are the administrative districts? Could you provide a plot?*

We revised the sentence and caption of Figure 1 as follows:

“The differences in wet removal rates depending on the measurement sites ~~and, and six~~ and six administrative districts (Figure 1c), and season) are discussed in Sect. 3.1 and 3.2, respectively.” (L100–102)

“(c) The location of administrative districts and ~~The~~ spatial distribution of the mean BC mass in the potential emission region, which is the highest BC mass grid of each trajectory. The BC mass was obtained by multiplying (a) the emission rates and (b) the residence time.”

8. p3. l.85: *Again, you estimate the scavenging coefficients from FLEXPART? Why? I sense that I might miss or misunderstand something.*

We replaced ‘estimated from’ with ‘validated with’ to clarify our research purpose. The wet scavenging coefficient is embedded in FLEXPART according to the pre-studied parameters. And the only way to verify those coefficients is a comparison between measured and simulated concentrations that comprises the uncertainty of emission inventories. However, for the first time, this study provides a more accurate assessment of scavenging coefficients that are widely used in many chemical models by excluding the uncertainty from emission inventories.

“... the wet scavenging coefficients for below- and in-cloud processing were ~~estimated from validated with the measured~~ wet removal rate by allocating the air mass location (such as below or within the cloud) and meteorological variables along the pathway of air mass transport.” (L103–105)

9. p.3 l.93: *What does “intensive” in this context mean? Do you really mean intensive?*

The official name for those sites operated by NIER is ‘Intensive Measurement Station’. We have changed the capital letters as follows:

“... one of the Intensive Measurement Stations ~~intensive measurement stations~~ operated by ...” (L112–113)

10. p.3 l.98: *“The measurement periods were mainly in the early 2010s . . . .”; Do you mean that they start in the early 2010s?*

As described in the caption of Figure S1, the measurement periods at three sites began in the early 2010s, e.g., 2010 for Baengnyeong, 2012 for Gosan, and 2011 for Noto. Despite the measurement periods being clarified in Figure S1, we added the measurement periods as follows:

“The longest measurement period was in Noto for approximately 6 years (from 2011 to 2016), followed by that in Baengnyeong (5 years; 2010 to 2017 except for 2011 to 2012) and Gosan (3 years; 2012 to 2015).” (L118–120)

11. p.3 l.99: *Since Figure S1 is in the supplement, you might want to add a note on that.*

Please refer to response #10.

12. p.3 l.101: *“well-validated” ; What is well-validated? There should be a criterion for this.*

We revised the sentence by adding the references for validation of the BC measurement as follows:

“In this study, we tried to obtain reliable BC concentrations from well-validated instruments, including OC–EC analyzers (Sunset Laboratory Inc., USA) with optical corrections, multi-angle absorption photometers (MAAPs; MAAP 5012, Thermo Scientific), and a continuous light absorption photometer (CLAP), yielding good agreement in the BC concentrations between the instruments (uncertainty  $\leq \pm 15\%$ , except for CLAP at  $\leq \pm 20\%$ ) (Choi et al., 2020; Kanaya et al., 2008, 2013; Miyakawa et al., 2016, 2017; Taketani et al., 2016).” (L121–125)

“The overall uncertainty of ~~BC and~~ CO measurements from different instruments was estimated to be less than ~~15% (except for Gosan; 20%) and 5%, respectively~~, which leads to a 10% uncertainty ~~of in the~~ overall regional  $\Delta BC/\Delta CO$  ratio (Choi et al., 2020).” (L136–138)

13. p.4 l.118: *Why mentioning GDAS?*

This statement clarified the use of ERA5 instead of GDAS, which is mainly used for HYSPLIT models, and emphasized that a much finer spatial resolution can provide more accurate backward trajectories compared to GDAS.

14. p.4 l.119: *Do the pressure levels correspond to ERA5 or GDAS?*

Yes, the pressure levels corresponded to GDAS, and those of ERA5 were described in L150. However, the pressure level of GDAS was deleted to improve the conciseness of the sentence as follows:

“... as input for HYSPLIT instead of Global Data Assimilation System (GDAS); ~~1°×1° data with 23 pressure levels~~) to improve the accuracy assessment of the air mass transportation pathways and to acquire more detailed information on the meteorological conditions.” (L145–147)

15. p.4 l.121: *Did you disaggregate the precipitation fields as they are done for Flexpart simulations? For better comparison to Flexpart results.*

We used both precipitation fields, large-scale (lsp) and convective precipitation (cp) as described in L326, and we also added a description of precipitation as follows:

“According to the pathway of air mass transportation, the detailed meteorological information, such as for precipitation (sum of large-scale and convective precipitation), and clouds, and so on, was acquired from ERA5 hourly data at both single and pressure levels (37 levels; 1000 hPa to 1 hPa) according to the HYSPLIT backward trajectories to identify the below and/or in-cloud cases and to calculate the wet scavenging coefficients.” (L148–153)

However, we did not interpolate the meteorological input data linearly to the position of computational particles in time and space (Hittmeir et al., 2018). Hittmeir et al. (2018) evaluated their new algorithms by comparing them with ECMWF 1 h data (0.5° resolution), which had a coarser resolution than used in the current study (0.25° resolution). In the case of HYSPLIT model, we considered the homogenous precipitation rate within a single grid cell because the temporal (1 h) and spatial resolution of ERA5 are dense enough to represent local variability compared to ERA-Interim (3 h with 1°). Moreover, the precipitation rates (lsp+cp) of HYSPLIT using ERA5 and FLEXPART using ERA-Interim showed negligible differences, thus justifying our results. A discussion of separating precipitation and uncertainty in the APT between the two datasets was included in Supplement S2 as follows:

“Figure S2 presents the cumulative probability of APT from HYSPLIT and FLEXPART. Although the air mass pathway showed insignificant differences between the two models, the median APT of FLEXPART (1.2 mm) was two times higher than that of HYSPLIT (0.63 mm), indicating a higher bias of the FLEXPART APT. This result can be caused by the difference in meteorological input data and the treatment of precipitation fields, homogeneous precipitation in a single grid cell (0.25°×0.25°) in HYSPLIT and disaggregated precipitation induced by interpolating in time and space in FLEXPART (Hittmeir et al., 2018). The higher bias in the FLEXPART APT contributed to increasing the magnitude of the underestimation of FLEXPART TE when assuming the same APT from HYSPLIT model, indicating an insignificant impact on the results.” (Sect. S2 in the Supplement)

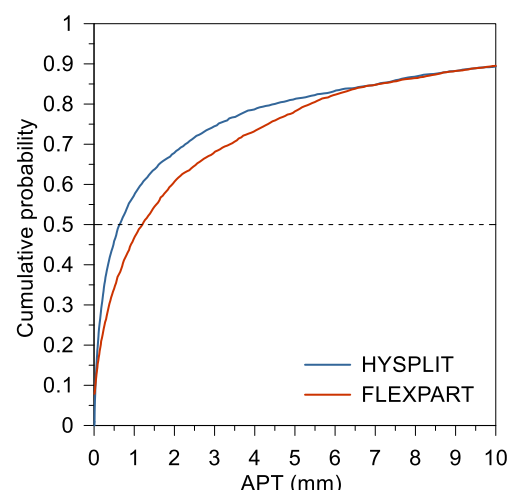


**Figure S2.** Cumulative probability plot of the APT from HYSPLIT (blue) and FLEXPART (red) during the study periods at the three sites. The dashed black line indicated a cumulative probability at 0.5 (median).

16. p.4 l.124: *What are the main BC regions? How is “main BC region” defined?*

The ‘main BC source region’ was intended to represent the highest BC-emitting region during air mass transport. We added a detail description of the main BC source region as follows:

“As the air mass was being transported, if precipitation occurred before the air mass arrived at the main BC source region, which is the highest BC emission area, it is difficult to investigate then the magnitude of wet removal effect as a function of APT could be underestimated at receptor sites because the air mass containing BC would not have been exposed to wet scavenging conditions effects of precipitation could be underestimated at receptor sites.” (L154–157)

17. p.4 l.125: *Why couldn’t the precipitation not be overestimated?*

This statement indicated the underestimation of wet scavenging by precipitation and not the amount of precipitation. If precipitation occurred before arriving at the main BC source region, the air mass containing BC would not have experienced wet scavenging, which may be misinterpreted as a reduced impact of wet scavenging. Moreover, Nogueira (2020) reported that ERA5 showed lower

bias and higher correlations with Global Precipitation Climatology Project (GPCP) compared to ERA-Interim at the mid-latitude regions. Please refer to our response to comment #16.

Nogueira, M.: Inter-comparison of ERA-5, ERA-interim and GPCP rainfall over the last 40 years: Process-based analysis of systematic and random differences, *Journal of Hydrology*, 583, 124632, <https://doi.org/10.1016/j.jhydrol.2020.124632>, 2020.

18. *p.5 l.150: What do the global models have to do with this study?*

The relevant sentence explained the reason for excluding the dry deposition effects in our analysis because the our estimated dry deposition velocity was even smaller by a factor of 3–10 compared with that used in various global models (such as NCAR CAM3, GISS GCM II-prime, MOZART-4, and so on). We revised the relevant sentence to specify the dry deposition velocity in global models and provided references as follows:

“Although TE is also affected by dry deposition, ~~but~~ Choi et al. (2020) reported that the effect of dry deposition could be ~~negligible~~ neglected because dry deposition velocities (0.01–0.03 cm s<sup>-1</sup>) are much lower than the default setting (0.1 cm s<sup>-1</sup>) in global models (Chung and Seinfeld, 2002; Cooke and Wilson, 1996; Emmons et al., 2010; Sharma et al., 2013)(~~Choi et al., 2020~~).” (L184-187)

19. *p.5 l.155: shouldn't there be a reference to the Flexpart v10.4 paper?*

We added Pisso et al. (2019) with Stohl et al. (2005). (L191)

20. *p.5 l.159: ERA-Interim is not an operational reanalysis. ERA-Interim was suspended and ERA5 is now operational!*

Thank you for correction. We deleted term of ‘operational’ as follows:

“The FLEXPART model was executed with ~~operational~~ reanalysis meteorological data from the ECMWF ERA-Interim at a spatial resolution of 1°×1° with 60 ~~full-vertical~~ model levels from surface up to 0.1 hPa.” (L195–196)

21. *p.5 l.159-160: You should rewrite to “60 model levels” since vertical levels could also be pressure levels or others.*

We revised the expression according to the reviewer’s suggestion.

“The FLEXPART model was executed with ~~operational~~ reanalysis meteorological data from the ECMWF ERA-Interim at a spatial resolution of 1°×1° with 60 ~~full-vertical~~ model levels from surface up to 0.1 hPa.” (L195-196)

22. *p. 5 l.160: “ECMWF has a resolution of 3h. . .” this is wrong. The ERA-Interim data set has this resolution, but not ECMWF in general.*

We revised the sentence as follows:

“Temporally, ~~ECMWF~~ ERA-Interim has a resolution of 3 h, with ~~6~~ 12 h analysis and 3 h forecast time steps.” (L197–198)

23. *p.5 l.168: what do you mean by “extracted” ? How do you calculate the TE with Flexpart data.*

By modifying the FORTRAN code (wetdepo.f90) to print out the wet scavenging coefficients of each grid cell, TE can be calculated from equations (2) and (3) in Sect. 3.3. To enhance the readability, we referred to Sect. 3.3, which contains more detailed information as follows:

“To validate the wet scavenging scheme in FLEXPART by comparison with the measured TE value, the wet scavenging coefficients for below- and in-clouds were extracted from FLEXPART to calculate TE (see Sect. 3.3 for more details).” (L204–206)

24. *p.5 l.174: Could you define the bins somewhere? This should be done according to be able to reproduce the results.*

We added a description of APT bins in the caption of Figure 2 as follows:

“The 9 bins consist of 0.01–0.25, 0.25–0.50, 0.50–0.75, 0.75–1.0, 1.0–2.5, 2.5–5.0, 5.0–10, 10–20, and 20–30 mm.”

25. p.5 l.178: *What was R2 before it was improved?*

We added the  $R^2$  value (0.940) from the widely used equation  $A-B \times \log(APT)$  as follows:

“..., because the coefficients of determination ( $R^2$ ) was improved from 0.940 ~~up~~ to 0.981 though TE values from three sites were used (Table 1).” (L219–220)

26. p.5 l.183: *This Fukue site comes out of nowhere and it is not clear where it is located.*

The results from Fukue were from a previous study; thus, we added the longitude and latitude of Fukue site as follows:

“The parameters  $A_1$  ( $0.269 \pm 0.039$ ) and  $A_2$  ( $0.385 \pm 0.035$ ) of the overall fitting were higher and lower, respectively, than the derived equation from the Fukue site ( $A_1 = 0.109$  and  $A_2 = 0.68$ ), which is a remote site in Japan (128.68° E, 32.75° N) (Kanaya et al., 2016).” (L222–224)

27. p.6 l.187: *I don't understand how the new SED indicates the transport to the Arctic, please explain further.*

Zhu et al. (2020) reported that the anthropogenic BC emitted from East Asia and Russia could contribute significantly to Arctic BC at surface level (62%; 56% for Russia and 6% for East Asia) and high altitudes (48%; 8% for Russia and 40% for East Asia) according to the FLEXPART model. The statement ‘transport to the Arctic’ means that the contribution of BC emitted from East Asia (also Russia) can be affected by the wet scavenging efficiency and our new derived SED indicated that reduced scavenging efficiency resulted in more transport of BC to the Arctic compared to Kanaya et al. (2016) “because  $A_2$  determines the magnitude of the wet removal efficiency according to APT” (L229). We revised the relevant sentence to more clearly convey our intended meaning as follows:

“In particular, the  $A_2$  value is important for calculating the TE-amount of BC from emission sources via ~~for~~ long-range transport, e.g., toward the Arctic (Kanaya et al., 2016; Zhu et al., 2020), because  $A_2$  determines the magnitude of the wet removal efficiency according to APT. Thus, the newly obtained SED equation, which has a low  $A_2$  value, indicates that more BC will ~~might~~ be transported to the Arctic region than previously that reported by Kanaya et al. (2016).” (L226–230)

28. p.6 l.214: *what global model?*

We revised the sentence as follows:

“This calculated  $e$ -folding lifetime in East Asia was much shorter than 16.0 days for BC from FLEXPART v10 ~~for the global model~~ (Grythe et al., 2017).” (L255–257)

29. p.7 l.224: “A similar tendency of  $R^2$ ,  $TE=0.5$  also showed .. “; *I don't understand this formulation. Do you mean  $R^2$  and TE?*”

We revised the sentence as follows:

“A similar tendency of  $R^2$ , the APTs to achieve  $TE=0.5$  also showed regional differences ~~different APTs~~, i.e., higher in East and North China and lower in other regions.” (L267–268)

30. p.8 l.258: *wasn't this described in Grythe et al. 2017?*

Grythe et al. (2017) also discussed  $f_g$ , although they did not include a detailed equation and constants for calculating  $f_g$ . Therefore, we only cited the study by Stohl et al. (2005).

31. p.8 l.258 – 261: *Its not only the grid resolution but the whole model physics is different apart from the differences between Hysplit and Flexpart. Additionally, regional/local pattern of precipitation*

and clouds are totally different especially because Flexpart uses disaggregated precipitation while it seems that Hysplit and ERA5 data used in this paper study weren't disaggregated. How does this reflect in the results? And why did you chose  $1^\circ \times 1^\circ$  for ERA-Interim instead of the  $0.75^\circ \times 0.75^\circ$  resolution ERA-Interim was stored on?

Please refer to our responses to comments #2 and #15. We used the default setting of 'flex\_extract' (FpExtractEcmwfData-7.0.2.tar.gz; available from <https://www.flexpart.eu/downloads>);  $1^\circ \times 1^\circ$  for ERA-Interim was the only option at that time.

32. p.8 l. 274.: In this section, I got confused by the values from measured vs ERA5 vs calculated vs reported vs Flexpart. Did you calculate the TE with the Flexpart scheme from ERA5 data? Then, what did you use from Flexpart simulation results?

Please refer to the main response and comment #4 in major comments.

33. p.8 l.301: again, could you please define the bins somewhere? (reproducibility)

We added a description of precipitation rate bins in the caption of Figure 5 as follows:

“The 11 bins consist of 0.01–0.04, 0.04–0.06, 0.06–0.08, 0.08–0.1, 0.1–0.2, 0.2–0.4, 0.4–0.6, 0.6–0.8, 0.8–1, 1–2, and 2–3 mm hr<sup>-1</sup>.”

34. p.8 l.307: what are reported values?

We revised the sentence as follows:

“Figure 6 shows the comparison of  $\Lambda_{\text{below}}$  ~~from reported values~~ calculated using equations from previous studies with ~~this study~~ that derived using our equation by assuming that the BC size was approximately 200 nm.” (L377–378)

35. p.8 l.319: could you give a reference for your statement of “the effect of differences in diameter might be negligible” please?

When we applied a larger diameter close to that of secondary ions (~ 500 nm) to the equation from Laakso et al. (2003),  $\Lambda_{\text{below}}$  increased only 30% compared with that of ~200 nm (Figure R1), resulting in a similar average MFB (from 1.64 to 1.54) with Xu et al. (2017). Thus, we added the following:

“For example, the  $\Lambda_{\text{below}}$  of secondary ions in Beijing (Xu et al., 2017) had the highest MFB (1.68), and although the diameter ranges were larger (~ 500 nm) than those of BC, the effect of differences in diameter might be negligible because significant difference in  $\Lambda_{\text{below}}$  between two diameters were not observed (less than 30%) when applied to Laakso et al. (2003).” (L389–392)

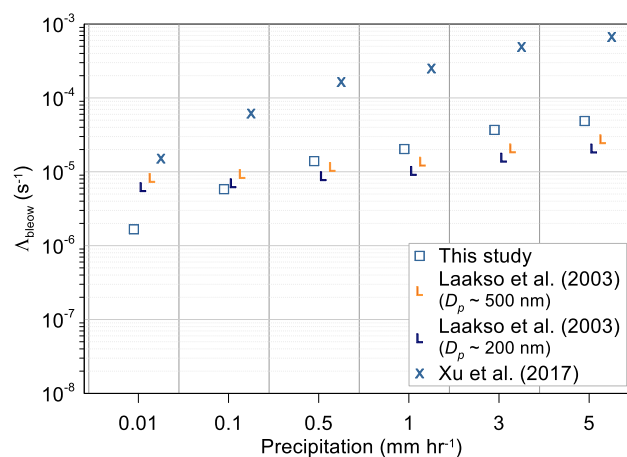


**Figure R1.** Same as Figure 6 except for adding the results obtained by applying a larger diameter (500 nm) instead of 200 nm in the equation from Laakso et al. (2003).

36. p.10 l.333: the Flexpart scavenging coefficient is taken from the simulations with ERA-Interim data and the estimated coefficient is from the measurement data in combination with the scheme from Flexpart and ERA5 data? Is this correct?

That is not correct. The FLEXPART scavenging coefficients ( $\Lambda$ ; now ‘calculated’  $\Lambda$ ) were calculated by HYSPLIT with ERA5 pressure level data according to the FLEXPART scheme. The estimated (now ‘measured’)  $\Lambda_{\text{in}}$  was calculated from the measured TE with HYSPLIT and ERA5. As mentioned in our main response, only the measured TE was compared with the simulated TE



from FLEXPART, and the measured below- and in-cloud scavenging coefficients were compared with those calculated according to the FLEXPART scheme (not simulated).

37. p10. l.362: *what would be the effect if it would be 4:1 or 2:1?*

When the training and test sample ratio was varied from 4:1 to 2:1, the relative importance in Figure 7b changed slightly, but CAPE was still the most important variable among the six input variables.

38. Table 2: *Does this mean Flexpart does not correspond to the ERA-Interim simulation results but to the calculated values with ERA5 data and the Flexpart scheme? If not, reformulate please.*

Please refer to the main response and comment #4 in major comments.

We revised the caption of Table 2 to clarify the meaning of  $\Lambda_{\text{below}}$  and  $\Lambda_{\text{in}}$  and replaced ‘FLEXPART’ with ‘calculated.’

**Table 3.** Summaries of the transport efficiency (TE) and scavenging coefficients for selected (a) below- and (b) in-cloud cases based on ERA5 hourly data of pressure levels from ECMWF.

Cases	Median	Interquartile range (25 <sup>th</sup> percentile – 75 <sup>th</sup> percentile)
(a) Below cloud ( $N_{\text{case}}=831$ )		
TE	0.89	[0.61 – 1.27]
<del>Estimated</del> <u>Measured</u> $\Lambda_{\text{below}}$ ( $\text{s}^{-1}$ )	$4.01 \times 10^{-6}$	$[2.70 \times 10^{-6} - 6.33 \times 10^{-6}]$
<del>FLEXPART</del> <u>Calculated</u> $\Lambda_{\text{below}}$ ( $\text{s}^{-1}$ ) <sup>a</sup>	$6.63 \times 10^{-6}$	$[6.38 \times 10^{-6} - 7.08 \times 10^{-6}]$
(b) In-cloud ( $N_{\text{case}}=769$ )		
TE	0.72	[0.43 – 1.06]
<del>Estimated</del> <u>Measured</u> $\Lambda_{\text{in}}^*$ ( $\text{s}^{-1}$ ) <sup>b</sup>	$8.06 \times 10^{-5}$	-
<del>FLEXPART</del> <u>Calculated</u> $\Lambda_{\text{in}}^*$ ( $\text{s}^{-1}$ ) <sup>a, b</sup>	$7.28 \times 10^{-6}$	-

<sup>a)</sup> Calculated using the FLEXPART scheme

<sup>ab)</sup> Overall median value

Technical corrections:

p.3 l.83: *Afterward* → *Afterwards*

This has been corrected. (L102)

p.5 l.150: *remove “but”*

This has been corrected. (L185)

p.5 l.150: *negligible* → *neglected*

This has been corrected. (L185)

p.5 l.153: *I would suggest to exchange the order of “model simulation” and “measured values”*

This has been corrected. (L189)

p.5 l.166: *were existed* → *were available*

This has been corrected. (L204)

p.7 l.223: *was varied* → *varied*

This has been corrected. (L266)

p.7 l.230: *“ than the dominant in-cloud . . . ”* → *than in the dominant ...*

We revised it as follows:

“...; therefore, the wet removal efficiency should be lower than that in the dominant in-cloud scavenging region.” (L273–274)

*p. 7 l. 249: simulation → simulations*

This has been corrected. (L317)

# Investigation of the wet removal rate of black carbon in East Asia: validation of a below- and in-cloud wet removal scheme in FLEXPART v10.4

Yongjoo Choi<sup>1</sup>, Yugo Kanaya<sup>1</sup>, Masayuki Takigawa<sup>1</sup>, Chunmao Zhu<sup>1</sup>, Seung-Myung Park<sup>2</sup>, Atsushi Matsuki<sup>3</sup>, Yasuhiro Sadanaga<sup>4</sup>, Sang-Woo Kim<sup>5</sup>, Xiaole Pan<sup>6</sup>, Ignacio Pizzo<sup>7</sup>

<sup>1</sup> Research Institute for Global Change, Japan Agency for Marine-Earth Science and Technology (JAMSTEC), Yokohama, 2360001, Japan

<sup>2</sup> Division of Climate & Air Quality Research, National Institute of Environmental Research, Kyungseo-dong, Seo-Gu, Incheon 404170, Korea

<sup>3</sup> Institute of Nature and Environmental Technology, Kanazawa University, Kanazawa 9201192, Japan

<sup>4</sup> Department of Applied Chemistry, Graduate School of Engineering, Osaka Prefecture University, 1-1 Gakuen-cho, Naka-ku, Sakai, Osaka 5998531, Japan

<sup>5</sup> School of Earth and Environmental Sciences, Seoul National University, Seoul 08826, Korea

<sup>6</sup> Institute of Atmospheric Physics, Chinese Academy of Sciences, Beijing, China

<sup>7</sup> NILU – Norwegian Institute for Air Research, Kjeller 2027, Norway

Correspondence to: Yongjoo Choi ([choingjoo@jamstec.go.jp](mailto:choingjoo@jamstec.go.jp))

## Abstract

Understanding the global distribution of atmospheric black carbon (BC) is essential to unveil its climatic effect. However, there are still large uncertainties regarding the simulation of BC transport due to inadequate information about the removal process. We accessed the wet removal rate of BC in East Asia based on long-term measurements over the 2010–2016 period at three representative background sites (Baengnyeong and Gosan in South Korea and Noto in Japan). The average wet removal rate, represented by transport efficiency (TE), i.e., the fraction of undeposited BC particles during transport, was estimated as ~~to be~~ 0.73 in East Asia from 2010 to 2016. According to ~~the relationship between~~ accumulated precipitation along trajectory ~~and TE~~, ~~TE~~ ~~the wet removal efficiency~~ was lower in East and North China, ~~where the industrial sector (thin coated) is dominant; in contrast, but higher~~ ~~that~~ in South Korea and Japan ~~showed higher values, implying the importance of the aging process and frequency of exposure to below- and in-cloud scavenging conditions during airmass transport due to the transport sector (thick coated), with emissions mainly from diesel vehicles.~~ ~~By the same token~~ ~~TE~~ ~~the wet scavenging~~ in winter and summer showed the highest and lowest ~~value~~ ~~efficiency~~, respectively, ~~although the lowest removal efficiency in summer was primarily associated with a reduced BC aging process because the in-cloud scavenging condition was dominant, depending on the dominant emission sectors, such as house heating (thick coated) and industry.~~ The average half-life and  $e$ -folding lifetime of BC were 2.8 and 7.1 days, respectively, which is similar to previous studies, but those values differed according to the geographical location and meteorological conditions of each site. Next, by comparing TE from the FLEXPART Lagrangian transport model (version 10.4), we diagnosed the scavenging coefficients ( $s^{-1}$ ) of the below- and in-cloud scavenging scheme implemented in FLEXPART. The overall median TE from FLEXPART (0.91) was overestimated compared to the measured value, implying underestimation of wet scavenging coefficients in the model simulation. The median of the ~~measured~~ below-cloud scavenging coefficient showed a lower value than that calculated ~~from~~ ~~according to~~ FLEXPART ~~scheme~~, by a factor of 1.7. On the other hand, the overall median of the ~~calculated~~ ~~FLEXPART~~ in-cloud scavenging coefficients ~~from~~ ~~FLEXPART~~ ~~scheme~~ was highly underestimated by 1 order of magnitude compared to the measured value. From ~~the~~ ~~an~~ analysis of artificial neural networks, the convective available potential energy, which is well known as an indicator of vertical instability, should be considered in the in-cloud scavenging process to improve the representative regional difference in BC wet scavenging over East Asia. For the first time, this study suggested an effective and straightforward evaluation method for

42 wet scavenging schemes (both below- and in-cloud) by introducing TE along with excluding effects from the inaccurate  
43 emission inventories.

## 44 1. Introduction

45 Black carbon (BC) is the most significant light-absorbing aerosol that can cause positive radiative forcing on climate change  
46 (Winiger et al., 2016; Myhre et al., 2013; Bond et al., 2013; Emerson et al., 2018). However, state-of-the-art models still have  
47 ~~a~~ limitations in evaluating the direct radiative forcing of BC because of the large model uncertainties in simulating BC  
48 concentrations (Xu et al., 2019; Bond et al., 2013; Samset et al., 2014; Wang et al., 2014a; Schwarz et al., 2010; Sharma et al.,  
49 2013). This can partly be attributed to the following three reasons: (1) inaccurate bottom-up emission inventory, (2) the  
50 complexity of BC hygroscopicity, and (3) an imprecise dry/wet deposition scheme. First, when estimating the impact of BC  
51 using global models, the results usually contain large uncertainties in BC emissions (Cooke and Wilson, 1996; Chung and  
52 Seinfeld, 2002; Stier et al., 2007) because BC is mainly contributed by scattered emission sources. Therefore, the uncertainty  
53 of BC emission rates is large compared to other species (e.g., SO<sub>2</sub>, NO<sub>x</sub>, and CO<sub>2</sub>) whose emissions are dominated by large  
54 sources (Kurokawa et al., 2013; Zheng et al., 2018). Without appropriate constraints on the emissions, removal cannot be well  
55 quantified. Second, although BC itself is hydrophobic immediately after emission, it is subsequently converted to possessing  
56 hydrophilic properties through the aging process, in which water-soluble compounds coat BC, and during atmospheric  
57 transportation (Moteki et al., 2007; Matsui et al., 2018), and finally acts as cloud condensation nuclei (Kuwata et al., 2007;  
58 Bond et al., 2013). Such conversion depends on the initial state of the BC along with atmospheric conditions (presence of other  
59 particles and gases) and it has high spatial and temporal variabilities (Vignati et al., 2010). Third, while BC particles are  
60 transported in the atmosphere, they can be removed by dry and/or wet deposition, including below-cloud (i.e., washout) and  
61 in-cloud (i.e., rainout) processes. Wet deposition of BC, whose contribution to total removal is 79% (Textor et al., 2006), is  
62 still challenging to predict BC concentrations in the atmosphere due to the difficulties of accurate evaluation of wet removal  
63 (Emerson et al., 2018; Bond et al., 2013; Lee et al., 2013). Specifically, the in-cloud process is more efficient and complicated  
64 than the below-cloud process because the nucleation removal of aerosol particles within clouds is thought to account for more  
65 than 5046 ± 50% of the aerosol/BC particle mass removal from the atmosphere globally, although this is dependent on the  
66 selected global model (Grythe et al., 2017; Textor et al., 2006). However, there is insufficient in-field detailed observations to  
67 explain and quantify the interactions between BC and cloud particles at the microscale, which hinders a better understanding  
68 of the physical processes (Ding et al., 2019).

69 Accompanied with the refinement of BC emission inventories over East Asia (Choi et al., 2020; Kanaya et al., 2016), wet  
70 removal rates have been one of the main topics a focal point to better predict BC behavior by using the term transport efficiency  
71 (TE), which is the observationally-determined fraction of undeposited BC particles during transport (e.g., Oshima et al., 2012;  
72 Kondo et al 2016), because TE shows a good relationship with accumulated precipitation along trajectory (APT; sum of  
73 precipitation over the past 72 h backward trajectory) (Choi et al., 2020; Kanaya et al., 2016) ~~TE has been proven to be a good~~  
74 ~~proxy for wet scavenging.~~ Moteki et al. (2012), which was further elaborated from Oshima et al. (2012), reported the first  
75 observational evidence of the size-dependent activation of BC removal over the Yellow Sea during the Aerosol Radiative  
76 Forcing in East Asia (A-FORCE) airborne measurement campaign in the spring of 2009. Kondo et al. (2016) demonstrated an  
77 altitude dependence, with typical decreasing size distributions at higher altitudes associated with wet removal from A-FORCE  
78 in winter 2013. Kanaya et al. (2016) elucidated the relationship between the wet removal rate of BC and accumulated  
79 precipitation along trajectory (APT) from long-term measurements (2009–2015) at Fukue, Japan. Miyakawa et al. (2017)  
80 reported the effects of BC aging related to in-cloud scavenging during transport on the alteration of the BC size distribution  
81 and mixing states during the spring of 2015 at the same location. Matsui et al. (2013) demonstrated that the difference in the  
82 coating thickness of BC particles depended on the growing process (condensation and coagulation), indicating that the  
83 coagulation process is necessary to produce thickly coated BC particles that are preferentially removed via the wet scavenging

84 process. Recently, numerous fine mode particles, including BC<sub>1</sub> from polluted areas scavenging in clouds were more  
85 pronounced in East Asia, not only at a local scale but also at a large regional scale (Liu et al., 2018), because high aerosol  
86 loading conditions are usually associated with ~~considerable significant~~ cloud cover, which results in a higher frequency of wet  
87 scavenging (Eck et al., 2018).

88 BC and carbon monoxide (CO) are byproducts of the incomplete combustion of carbon-based fuels, and the ratio between  
89  $\Delta$ BC (the difference from the baseline level) and  $\Delta$ CO ~~could be is~~ a useful parameter for characterizing ~~combustion fuel~~ types.  
90 ~~due to because of their different carbon contents~~ (Zhou et al., 2009; Guo et al., 2017). Adopting APT, a useful index for the  
91 strength of wet deposition (Kanaya et al., 2016; Kanaya et al., 2020), the magnitude of the BC wet removal rate ~~according to~~  
92 ~~precipitation~~ can be easily characterized by the relationship between TE and APT. Although some previous studies have  
93 investigated wet scavenging schemes in models (Grythe et al., 2017; Croft et al., 2010), those results without well-constrained  
94 emission rates contain large ambiguity when assessing the wet deposition term (Vignati et al., 2010) ~~may include bias due to~~  
95 ~~the effect of inaccurate emission rate because emission rates and deposition terms were not necessarily separated~~. For the first  
96 time, the emission and deposition terms are distinctly separated in this study by introducing TE and using backward  
97 simulations,; this allows; thus allowing for the wet scavenging scheme to be evaluated more accurately because backward  
98 simulations do not account for the emission rate. By elaborating the regional  $\Delta$ BC/ $\Delta$ CO ratio (Choi et al., 2020), this study  
99 investigates the characteristics of the BC wet removal rate over East Asia using long-term measurements (more than 3 years)  
100 ~~with the best effort~~ to acquire reliable BC concentrations with wide spatial coverage over East Asia. The differences in wet  
101 removal rates depending on the measurement sites ~~and; and six~~ administrative districts (Figure 1c) and season) are discussed  
102 in Sect. 3.1 and 3.2, respectively. Afterwards, to evaluate the representativeness of the scavenging scheme in the recently  
103 updated FLEXible PARTicle dispersion model (FLEXPART) version 10.4, the wet scavenging coefficients for below- and in-  
104 cloud processing were ~~estimated-validated from with~~ the measured wet removal rate by allocating the air mass location (such  
105 as below or within clouds) and meteorological variables along the pathway of air mass transport.

## 106 2. Methods

### 107 2.1 Measurement sites and instruments

108 To investigate wet removal rates of the outflow air mass from China and Korea peninsula, BC and CO data from three  
109 measurement sites (Baengnyeong, Gosan in Korea and Noto in Japan; Figure 1a) were carefully selected for this study by  
110 considering major emission sources near the measurement sites and by obtaining reliable BC concentrations from different  
111 instruments. ~~As-Because~~ detailed information on the measurement sites and instruments is described in Choi et al. (2020), we  
112 only address brief information here. Baengnyeong (124.63°E, 37.97°N), one of the Intensive Measurement Stations ~~intensive~~  
113 ~~measurement stations~~ operated by the Korean Ministry of Environment, is frequently affected by airmasses from China  
114 (including East, North, and Northeast China) and North Korea. Gosan (126.17°E, 33.28°N) is located in the southern part of  
115 Korea and is frequently affected by airmasses from East China and South Korea. BC and CO were also measured at the Noto  
116 Ground-based Research Observatory (NOTOGRO, 137.36°E, 37.45°N), located on the Noto Peninsula on the western coast of  
117 Japan, which is frequently affected by airmasses from Northeast China and Japan. The measurement periods were mainly in  
118 the early 2010s but slightly different depending on the sites (Figure S1). The longest measurement period was in Noto for  
119 approximately 6 years (from 2011 to 2016), followed by that in Baengnyeong (5 years; 2010 to 2017 except for 2011 to 2012)  
120 and Gosan (3 years; 2012 to 2015).

121 In this study, we tried to obtain reliable BC concentrations from well-validated instruments, including OC-EC analyzers

(Sunset Laboratory Inc., USA) with optical corrections, multi-angle absorption photometers (MAAPs; MAAP 5012, Thermo Scientific), and a continuous light absorption photometer (CLAP), yielding good agreement in the BC concentrations between the instruments (uncertainty  $\leq \pm 15\%$ , except for CLAP at  $\leq \pm 20\%$ ) (Choi et al., 2020; Kanaya et al., 2008, 2013; Miyakawa et al., 2016, 2017; Taketani et al., 2016). ~~As the best effort to obtain reliable BC concentrations from different instruments, only well validated instruments were used in this study.~~ Hourly PM<sub>2.5</sub> elemental carbon (EC) was measured by a Sunset EC/OC analyzer with optical correction for Baengnyeong. ~~Multi-angle absorption photometer (A MAAP-5012)~~ was used to measure hourly BC in PM<sub>2.5</sub> ~~for at~~ Noto. At Gosan, BC in PM<sub>1</sub> was monitored by ~~a continuous light absorption photometer (a CLAP)~~ with three wavelengths including 467, 528, and 652 nm and the absorption was corrected following Bond (1999). At Noto, an improved mass absorption efficiency (MAE) of 10.3 m<sup>2</sup> g<sup>-1</sup> instead of the default value (6.6 m<sup>2</sup> g<sup>-1</sup>) was applied to estimate the BC mass concentration, as suggested based on calibrations using the thermal/optical method and the laser-induced incandescence technique (Kanaya et al., 2013; Kanaya et al., 2016). The CLAP also showed a good correlation with the co-located PM<sub>2.5</sub> EC concentrations from the Sunset EC/OC analyzer and the best-fit line was close to one (1.17), which is similar or slightly lower than the range of reported uncertainty of ~25% (Ogren et al., 2017). Hourly CO concentrations were measured by a gas filter correlation CO analyzer (Model 300 EU Teledyne Inc.) at Baengnyeong and by a nondispersive infrared absorption photometer (48C, Thermo Scientific) at the other two sites. The overall uncertainty of ~~BC and~~ CO measurements from different instruments was estimated to be less than ~~15% (except for Gosan; 20%) and 5%, respectively,~~ which leads to a 10% uncertainty ~~of in the~~ overall regional  $\Delta BC/\Delta CO$  ratio (Choi et al., 2020).

## 2.2 Backward trajectory and meteorological data

To identify the air mass origin region, 5 d (72–120 h) backward trajectories were calculated four times a day (00, 06, 12, 18 UTC) using the Hybrid Single Particle Lagrangian Integrated Trajectory (HYSPPLIT) Model version 4 (Draxler et al., 2018). The starting altitude was 500 m above ground level (AGL). The past 120 h of backward simulation time was selected by considering the lifetime of BC (~5 d; Lund et al., 2017, 2018; Park et al., 2005). It should be noted that the different starting altitude (500 m vs. 1000m) did not impact on our results (Sect. S1 in the Supplement). Notably, we used the European Centre for Medium-Range Weather Forecasts (ECMWF) ERA5, which provides a much finer resolution of 0.25°×0.25°, as input for HYSPPLIT instead of Global Data Assimilation System (GDAS); ~~1°×1° data with 23 pressure levels~~ to improve the accurate assessment of the air mass transportation pathways and to acquire more detailed information on the meteorological conditions. According to the pathway of air mass transportation, the detailed meteorological information, such as ~~for~~ precipitation (sum of large-scale and convective precipitation), and clouds, and so on, was acquired from ERA5 hourly data at both single and pressure levels (37 levels; 1000 hPa to 1 hPa) ~~to identify the below and/or in cloud cases and to calculate the wet scavenging coefficients.~~ By considering the vertical height of the air mass from the HYSPPLIT model and cloud information from ERA5, we successfully distinguished the dominant cases for below-cloud (no residence time within cloud) and in-cloud (no residence time below cloud) cases when precipitation  $\geq 0.01$  mm hr<sup>-1</sup> and calculated the wet scavenging coefficients.

As the air mass was being transported, ~~if~~ precipitation occurred before the air mass arrived at the main BC source region, which is the highest BC emission area, it is difficult to investigate then the magnitude of wet removal effect as a function of APT could be underestimated at receptor sites because the air mass containing BC would not have been exposed to wet scavenging conditions ~~effects of precipitation could be underestimated at receptor sites~~. Therefore, we considered the residence time (Li et al., 2014; Ashbaugh et al., 1985) of each grid cell (0.25°×0.25°) and the BC emission rates (mass time<sup>-1</sup>) from the Regional Emission inventory in ASia (REAS; Figure 1a) emission inventory (Kurokawa et al., 2013) version 2.1 to identify the potential emission region by multiplying residence time and emission rates. First, when the air mass altitude was lower than

2.5 km, the air mass velocities ( $V_n$  and  $V_{n+1}$ ) were calculated by distances from the central point in a target grid cell to two-way endpoints of backward trajectories ( $D_n$  and  $D_{n+1}$ ) using  $V_n = D_n / \Delta t$  and  $V_{n+1} = D_{n+1} / \Delta t$  (Figure 1b), where  $\Delta t$  and  $n$  represent the time interval of meteorological data (1 h) and  $n$ th grid cell, respectively. Then, by assuming that the air mass velocity is constant within the time interval, the residence time in a grid cell ( $T_{grid}$ ) was calculated by considering both the distance of each grid corner ( $d_n$  and  $d_{n+1}$ ) and the corresponding velocities ( $V_n$  and  $V_{n+1}$ ) using  $d_n / V_n + d_{n+1} / V_{n+1}$ . Based on the identified potential emission region, APT was recalculated only after the air mass passed through the potential emission region when precipitation occurred when APT over the past 72 h was higher than 0. Figure 1c reveals the geographical distribution for the mean BC mass of identified potential emission regions, indicating that this approach was appropriate because of good spatial coverage the potential emission regions were uniformly distributed over East Asia, including East China, a major emission source for BC. We checked the uncertainty arising from selecting different criteria for altitude (1.5 km), but there was no significant difference in the results (Sect. S1 in the Supplement).

### 2.3 Transport efficiency (TE)

The TE of BC is defined as the ratio of the BC and CO concentrations measured at the receptor site to that anticipated if there was no wet removal during transport (i.e., APT during past 72 h is zero). Thus, the TE of the air mass was calculated by eq. (1),

$$TE = \frac{[\Delta BC / \Delta CO]_{APT > 0}}{[\Delta BC / \Delta CO]_{APT = 0}} \quad (1)$$

where delta ( $\Delta$ ) indicates the difference between BC and CO concentrations and their baseline concentrations (Moteki et al., 2012; Oshima et al., 2012; Kanaya et al., 2016). The baseline CO was estimated as a 14-day moving 5th percentile from the observed CO mixing ratio, but the BC baseline was regarded as zero because the atmospheric lifetime of BC is known as several days, which is much shorter than that of CO (1–2 months).  $[\Delta BC / \Delta CO]_{APT = 0}$  indicated the regional median value of  $\Delta BC / \Delta CO$  under dry conditions implying the original emission ratio. In our previous work, we successfully elucidated that  $[\Delta BC / \Delta CO]_{APT = 0}$  depends on the regional characteristics of the energy consumption types (Kanaya et al., 2016; Choi et al., 2020). The decrease in the ratio with APT,  $[\Delta BC / \Delta CO]_{APT > 0}$ , was related to BC-specific removal due to wet scavenging processes and thus the TE was-is an effective indicator to investigate the wet removal process. Although TE is also affected by dry deposition, but Choi et al. (2020) reported that the effect of dry deposition could be negligible-neglected because dry deposition velocities ( $0.01\text{--}0.03 \text{ cm s}^{-1}$ ) are much lower than the default setting ( $0.1 \text{ cm s}^{-1}$ ) in global models (Chung and Seinfeld, 2002; Cooke and Wilson, 1996; Emmons et al., 2010; Sharma et al., 2013) (Choi et al., 2020).

### 2.4 FLEXPART model

To compare the wet-removal-rates TE between the model-simulation-and measured values and model simulation, the FLEXPART v10.4 was used to simulate BC wet scavenging over East Asia using the backward mode. Detailed information for the FLEXPART is readily found in the literature (e.g., Pisso et al., 2019 and Stohl et al., 2005); thus, we only briefly describe the information here. The FLEXPART version 10.4 was-is the official version to allow turning on the wet scavenging module in the backward simulation mode (<https://www.flexpart.eu/downloads>, obtained 10 October 2019). The equations and detailed description for-of the below- and in-cloud scavenging scheme are explained in Pisso et al. (2019) and Grythe et al. (2017). The FLEXPART model was executed with operational reanalysis meteorological data from the ECMWF ERA-Interim at a spatial resolution of  $1^\circ \times 1^\circ$  with 60 full-vertical-model levels from surface up to 0.1 hPa. Temporally, ECMWF-ERA-Interim has a resolution of 3 h, with 612 h analysis and 3 h forecast time steps. The period and daily frequency of simulation



were the same as those of the HYSPLIT model (past 72 h and four times, respectively). The grid resolution of FLEXPART was also same with ECMWF ERA-Interim ( $1^{\circ}\times 1^{\circ}$ ). It should be noted that chemistry and microphysics could not be resolved by the FLEXPART. The FLEXPART model, therefore, ignores the aging process (from hydrophobic to hydrophilic state changes and size changes of BC) and assumes that all BC particles are aged hydrophilic particles. A logarithmic size distribution of BC with a mean diameter of 0.16  $\mu\text{m}$  and a standard deviation of 1.84, in accordance with measurement in Japan, was used (Miyakawa et al., 2017). A total of  $10^4$  particles were randomly released at 500 m from each receptor site during 1 h when the measurement data were ~~existed~~ available. To validate the wet scavenging scheme in FLEXPART by comparison with the measured TE value, the wet scavenging coefficients for below- and in-clouds were extracted from FLEXPART to calculate TE (see Sect. 3.3 for more details). Note that the simulated TE from FLEXPART (FLEXPART TE) was only used for comparing with the measured TE. Despite the difference in the input meteorological fields between HYSPLIT and FLEXPART, the difference in air mass pathways and APT between two datasets can be neglected (Hoffmann et al., 2019; Sect. S2 in the Supplement).

## 3 Results

### 3.1 Overall variation of transport efficiency (TE)

Figure 2 shows that measured  $[\Delta\text{BC}/\Delta\text{CO}]_{\text{APT}=0}$  (left panel) and TE variations (right panel) depend on APT and the measurement sites. The overall median  $[\Delta\text{BC}/\Delta\text{CO}]_{\text{APT}=0}$  was  $6.4 \text{ ng m}^{-3} \text{ ppb}^{-1}$ , which converged from Baengnyeong ( $6.2 \text{ ng m}^{-3} \text{ ppb}^{-1}$ ), Gosan ( $6.5 \text{ ng m}^{-3} \text{ ppb}^{-1}$ ) and Noto ( $6.7 \text{ ng m}^{-3} \text{ ppb}^{-1}$ ), indicating that TE is characterized by a regional  $[\Delta\text{BC}/\Delta\text{CO}]_{\text{APT}=0}$  per site. We divided APT into 9 range bins and applied exponential fitting equations to quantify the wet removal process. Among  $N_{\text{APT}>0}$  (total number of data points when  $\text{APT} > 0 \text{ mm}$ ), only the data point fraction in each bin to  $N_{\text{APT}>0} \geq 2\%$  was considered to secure the statistic. It should be noted that we found the relationship between TE and APT by using the stretched exponential decay (SED) equation,  $\exp(-A_1 \times \text{APT}^{A_2})$ , instead of the widely used equation,  $A \times \log(\text{APT})$ , because the coefficients of determination ( $R^2$ ) was improved ~~up from 0.940~~ to 0.981 though TE values from three sites were used (Table 1). This fitting equation is normally used to describe below-cloud scavenging, whereas wet removal of BC is generally believed to be dominated by in-cloud rather than below-cloud processes because of the small size of BC-containing particles. Therefore, the equations should contain both below- and in-cloud scavenging effects. The parameters  $A_1$  ( $0.269 \pm 0.039$ ) and  $A_2$  ( $0.385 \pm 0.035$ ) of the overall fitting were higher and lower, respectively, than the derived equation from the Fukue site ( $A_1 = 0.109$  and  $A_2 = 0.68$ ), which is the remote site in Japan ( $128.68^{\circ} \text{ E}$ ,  $32.75^{\circ} \text{ N}$ ) (Kanaya et al., 2016). It can be easily deduced that the wet removal effect at the three sites was initially more effective than that at Fukue, but the wet removal effect at Fukue gradually accelerated as the APT increased. In particular, the  $A_2$  value is important for calculating the ~~TE amount~~ of BC from emission sources for ~~via~~ long-range transport, e.g., toward the Arctic (Kanaya et al., 2016; Zhu et al., 2020), because  $A_2$  determines the magnitude of the wet removal efficiency according to APT. Thus, the newly obtained SED equation, which has a low  $A_2$  value, indicates that more BC will-might be transported to the Arctic region than ~~previously~~ that reported by Kanaya et al. (2016).

The decreasing pattern of median TE for Baengnyeong did not closely follow the overall SED and had a much lower  $R^2$  (0.77), indicating that the wet removal process at Baengnyeong could not simply be expressed by APT. In contrast, the  $R^2$  of Gosan and Noto were sufficiently high to represent the wet removal characteristics. The aging process due to different traveling times might be one of the reasons. Because long-range transported BC has a larger core diameter than BC from local sources (Lamb et al., 2018; Ueda et al., 2016), these larger BC cores are preferentially removed via the wet scavenging process (Moteki

et al., 2012). ~~However, p~~Previous studies reported that the mass median diameter (MMD) of refractory BC (rBC) at Baengnyeong, Gosan, and Noto in spring were 218, 196, and 200 nm, respectively (Oh et al., 2015; Ueda et al., 2016; Oh et al., 2014) indicating much more aging compared with local emissions in Seoul, South Korea (180 nm) and Tokyo, Japan (163 nm) (Park et al., 2019; Ohata et al., 2019). In addition, the difference in the wet removal rate depending on measurement sites could be partly explained by ~~the differences~~ in meteorology. The monthly mean meteorological parameters indicated that Baengnyeong has characteristics of low precipitation (80.6 mm), cloud cover (0.57), total column cloud water ( $0.06 \text{ kg m}^{-2}$ ), and high cloud bottom height (2.5 km) compared to other sites, suggesting the lower exposure time to both below- and/or in-cloud condition during ~~the transportation~~ (Figure 3). In contrast, ~~the SED fittings for~~ both Gosan and Noto showed similar ranges of high precipitation (127 and 174 mm), total cloud cover (0.65 and 0.64), and total column cloud water ( $0.09$  and  $0.12 \text{ kg m}^{-2}$ ) but low cloud bottom height (1.9 and 2.0 km), respectively. In addition, the ~~different BC coating thicknesses according to the emission source and fuel types could also contribute to the site difference of the wet removal rate, which difference in magnitude of aging BC and frequency of exposure to below- and in-cloud scavenging conditions~~ will be further discussed in Sect. 3.2.

Using the overall SED fitting equation, TE at 0.5 ( $TE=0.5$ ) and  $e$ -folding ( $TE=1/e$ ) could be reached when the APT values were 11.7 and 30.2 mm, respectively (Table 1). Similar to the SED results, Baengnyeong needed much higher precipitation of 70.9 and 202 mm to reach  $TE=0.5$  and  $TE=1/e$ , respectively, but the other sites showed lower APTs of 16.4 mm and 42.3 mm for Gosan and 8.0 mm and 20.3 mm for Noto, respectively. Considering the annual mean precipitation at the three sites (1542 mm), it took 2.8 and 7.1 days to reach  $TE=0.5$  and  $TE=1/e$ , respectively. Kanaya et al. (2016) reported a similar half-life and shorter  $e$ -folding lifetime for BC at Fukue ( $2.3 \pm 1.0$  and  $4.0 \pm 1.0$  days, respectively), calculated from the  $15.0 \pm 3.2$  mm and  $25.5 \pm 6.1$  mm of APT to reach  $TE=0.5$  and  $TE=1/e$ , respectively, along with annual precipitation, 2335 mm. This calculated  $e$ -folding lifetime in East Asia was much shorter than 16.0 days for BC from FLEXPART v10 ~~the global model~~ (Grythe et al., 2017).

Based on a similar approach over the Yellow Sea using an aircraft-borne single particle soot photometer (SP2) during the A-FORCE campaign (Oshima et al., 2012), attaining  $TE=0.5$  required different magnitudes of APT depending on not only the air mass origin but also the altitude. These authors also reported that the TE of northern China was higher than that of southern China regardless of altitude. Therefore, in the next section, we will further investigate why the difference in halving or  $e$ -folding lifetimes depends on region and season by analyzing the differences in the origin pathway of air masses ~~and the seasonal variation of BC emission sources~~.

### 3.2 Regional and seasonal variations of the transport efficiency (TE)

Figure 4 indicates the variation of TE depending on the potential source regions (hereafter regions) and seasons. The  $R^2$  for each ~~source~~-region ~~was~~ varied from 0.656 to 0.945 and was lower in East and North China and North Korea and higher in other regions (Table 1). A similar tendency of  $R^2$ , the APTs to achieve  $TE=0.5$  also showed regional differences ~~different APTs~~, i.e., higher in East and North China and lower in other regions. The regional differences in wet removal efficiency can partly be attributed to the following reasons.

First, the transport pathway of air masses from East and North China could be less exposed to in-cloud scavenging than other regions because the most of potential emission source in East and North China is located over  $30^\circ\text{N}$  (Figure 1c), which has low cloud cover and water contents along with high cloud bottom heights (Figure 3). Although the amount of APT was similar to that in other regions, it was mostly composed of below-cloud scavenging; therefore, the wet removal efficiency should be lower than that in the dominant in-cloud scavenging region. To quantify the effect of below- and in-cloud scavenging, we

investigated the fraction of exposure to below- and in-cloud scavenging conditions during the air mass transport according to regions. Among the total frequency of grid cells which air mass passed (~500,000), ~25% of the grid cells were exposed to below- (~10%) and in-cloud scavenging conditions (~15%), indicating that the in-cloud conditions were relatively predominant in wet scavenging over East Asia. The higher wet removal efficiency region (South Korea and Japan) revealed an apparently higher fraction of exposure to below- (~11%) and in-cloud scavenging conditions (~19%) compared to the air mass from East and North China (~8% for below- and ~10% for in-cloud scavenging condition), suggesting the importance of in-cloud scavenging process for wet deposition.

Second, the difference in the degree of BC aging process could be an important factor for determining the wet scavenging efficiency. Freshly emitted BC particles have small diameters, exhibit a thin coating thickness, and are hydrophobic; thus, they would not be effective in wet scavenging compared to aged BC particles. Typically, the coefficient of BC aging rate in North China Plain was significantly higher than that used in previous models (e.g., Cooke and Wilson, 1996; Koch and Hansen, 2005; Xu et al., 2019) due to the highly polluted environments (Zhang et al., 2019); however, the coefficients over East Asia are still unknown. In addition, the median regional traveling time of air masses to each site (11–47 h for Baengnyeong; 18–37 h for Gosan; 19–62 h for Noto) was different. Therefore, the difference in both the level of BC aging coefficient and traveling time depending on the region, which can influence the coating thickness of BC particles, might be another plausible reason underlying the regional differences in the wet removal efficiency. The difference in the coating thickness of BC particles, depending on the emission sectors, could be a major factor causing the difference in the wet removal efficiency because thickly-coated BC particles are much easier to remove by wet scavenging than less coated and/or freshly emitted BC (Ding et al., 2019; Miyakawa et al., 2017; Moteki et al., 2012). Typically, BC emitted from industrial regions, transport from diesel vehicles, and domestic sectors has characteristics of weakly, moderate, and strongly coated BC, respectively (Han et al., 2019; Liu et al., 2019), based on insignificant differences in the MMD of BC from those emission sectors (190–200 nm). This result coincided with the major emission sector of the REAS emission inventory in East and North China and North Korea (~57.5% emitted from industrial sectors) compared to other sites (12%–39%). In contrast, Northeast China showed low APT for reaching  $TE=0.5$  and  $TE=1/e$  because the dominant BC emission sector was residential sector (48.3%) which has a thickly coated characteristic. BC from South Korea and Japan reached  $TE=0.5$  and  $TE=1/e$  with a small amount of APT because moderately coated BC was mostly emitted from the transport sector (73.4%), mainly from diesel vehicles. It should be noted that the dominant emission sectors of industry (for East and North China and North Korea) or transport sectors (South Korea and Japan) were also confirmed by the Emission Database for Global Atmospheric Research (EDGAR) in 2010 and MIX in 2010 (Li et al., 2017; Crippa et al., 2018).

By the same token, in the case of seasonal variation in wet removal efficiency, the decreasing magnitude of  $TE$  according to APT was obviously emphasized in fall and winter, which was much steeper than that in spring and summer (Figure 4b). This tendency was reflected differences in not only the degree of aging process, but also the fraction of exposure to below- and in-cloud scavenging conditions. The fraction of below- and in-cloud scavenging in spring were lower at ~7% and ~11%, respectively, compared to those in fall and winter (11% for below- and 16% for in-cloud scavenging conditions). The fraction of in-cloud scavenging cases was the highest in summer (17%) compared to the other seasons, but the APT for reaching  $TE=0.5$  was also high, indicating that the removal efficiency of in-cloud scavenging was reduced. Considering the less pollution in summer, the lowest wet removal efficiency might be fully explained by the low coefficient of BC aging rate compared to that in other seasons (Zhang et al., 2019). In the effect of the residential sector, which has thickly coated BC, which increased due to house heating as the temperature decreased. In contrast to winter, the APT for reaching  $TE=0.5$  in spring and summer was the highest among the seasons. This might be caused by the increasing fraction of BC from the industrial sector in China while

315 ~~decreasing emissions from residential sectors (Kurokawa et al., 2013).~~

### 316 3.3 Comparison of measured and FLEXPART-simulated TE

317 In this section, by extracting the wet scavenging coefficients ( $\Lambda$ ;  $s^{-1}$ ) from the FLEXPART simulations, the difference in TE  
318 between the measured and simulated values was investigated. The scavenging coefficient ( $\Lambda$ ;  $s^{-1}$ ) is defined as the rate of  
319 aerosol washout and/or rainout due to the wet removal process. The TE value based on measurements and FLEXPART can be  
320 expressed by multiplying each TE ( $1 - \text{removal rate}$ ) of serial grid cells as in eq. (2),

$$321 TE = (1 - \eta_1)(1 - \eta_2) \cdots (1 - \eta_n) \quad (2)$$

322 where  $\eta_n$  indicates the removal rate in the  $n$ th grid cell and is expressed as in eq. (3),

$$323 \eta = [1 - \exp(-\Lambda \cdot t)] \cdot f_g \quad (3)$$

324 where  $t$  and  $f_g$  indicate the residence time and fraction for the subgrid in a grid cell, respectively. Because the precipitation is  
325 not uniform in a single grid cell,  $f_g$  accounts for the variability of precipitation in a grid cell in FLEXPART.  $f_g$  is a function of  
326 large-scale and convective precipitation, as described in Stohl et al. (2005). Although the grid resolution of the input  
327 meteorological data for the HYSPLIT model ( $0.25^\circ \times 0.25^\circ$ ) is much finer than that for FLEXPART ( $1^\circ \times 1^\circ$ ), we assumed the  
328 same potential emission region as the HYSPLIT model for calculating TE because there was no significant difference in the  
329 air mass pathway between the two outputs as we discussed in Sect. S2 in the Supplement.

330 The overall median ~~value~~ of measured TE was 0.72, and Baengnyeong showed the highest (0.88), followed by Gosan (0.70)  
331 and Noto (0.68) due to reasons explained in the previous sections. In comparison, the overall median ~~value~~ of FLEXPART TE  
332 (0.91) was much higher than the measured TE, indicating that the wet scavenging coefficients in the FLEXPART scheme were  
333 significantly underestimated. Moreover, the differences in FLEXPART TE depending on the measurement sites (0.95 for  
334 Baengnyeong, 0.94 for Gosan, and 0.87 for Noto) was not as large as the measured TE, suggesting that the regional differences  
335 in meteorological variables were relatively normalized and that the influence of other variables, which were not considered in  
336 the wet scavenging scheme, might be excluded in the calculation. Meanwhile, it is difficult to capture the local variation from  
337 coarse grid sizes, despite the air mass transport pathway between the two models being similar, because the key variables for  
338 determining the wet scavenging coefficient (such as precipitation, cloud cover, and so on) could have a large local variability.  
339 In addition, this approach still had a limitation in determining whether the overestimation of TE was resulting from the below-  
340 or in-cloud scavenging processes. Nevertheless, with similar rationale, further comparison of measured and ~~simulated~~  
341 calculated scavenging coefficients processes according to FLEXPART scheme could provide information to better represent  
342 wet removal schemes.

### 343 3.4 Below-cloud scavenging efficiency ( $\Lambda_{\text{below}}$ )

344 From this section, we aimed to investigate the below- and in-cloud scavenging in detail by discriminating the representative  
345 cases according to cloud information from the ERA5 pressure level data with HYSPLIT backward trajectory to overcome the  
346 limitation of the local variability of meteorological input variables. By considering distinguishing the dominant cases for below-  
347 and in-cloud vertical height of the air mass from the HYSPLIT model and cloud information from ERA5, we successfully  
348 distinguished the dominant cases for below cloud (no residence time within cloud) and in cloud (no residence time below  
349 cloud) cases, when precipitation  $\geq 0.01 \text{ mm hr}^{-1}$ , we compared our measured scavenging coefficients with those calculated  
350 according to FLEXPART scheme (not simulated). The median measured TE and residence time for only in-cloud cases (0.72

351 and  $\sim 7,200$  h) were much lower and longer, respectively, than those for only below-cloud cases (0.89 and  $\sim 5,100$  h), indicating  
 352 that in-cloud scavenging process is more efficient for wet removal of BC particle mass (Table 2). In the case of below-cloud  
 353 scavenging, the deviation of TE from unity could be simply converted to the scavenging coefficient ( $\Lambda_{\text{below}}$ ) by considering the  
 354 precipitation intensity, raindrop size, aerosol size, and residence time in a grid cell. Because many studies have made an effort  
 355 to parameterize  $\Lambda_{\text{below}}$  using observation data and/or the theoretical calculations (Xu et al., 2017; Wang et al., 2014b; Feng,  
 356 2007), we also parameterized this coefficient using a simplified method by following the scheme of below-cloud scavenging  
 357 in FLEXPART v10.4 (Laakso et al., 2003), which only considers the precipitation rate and aerosol size. Assuming a BC size  
 358  $\sim 200$  nm, TE for below-cloud can be expressed using equations (2) and (3) by substituting  $\Lambda$  with  $\Lambda_{\text{below}}$ , which depends only  
 359 on the precipitation rate in the subgrid cell ( $I_{\text{total}}$ ; the ratio of precipitation to  $f_g$ ). Because  $\Lambda_{\text{below}}$  can be determined by  
 360 constraining the proportion to the summation of  $I_{\text{total}}$ , hourly  $\Lambda_{\text{below}}$  from the sequential grid cell in a single case can easily be  
 361 obtained by minimizing  $\chi^2$ ,  $(\text{TE}_{\text{measured}} - \text{TE}_{\text{calculated}})^2$  when  $\chi^2 < 0.1$ . This was conducted using an R function for optimization  
 362 (optim; <https://stat.ethz.ch/R-manual/R-devel/library/stats/html/optim.html>), included in the standard R package “stats”.

363 Figure 5a indicates the empirical cumulative density function for the measured  $\Lambda_{\text{below}}$  from 869 cases. Although a substantial  
 364 fraction of  $\Lambda_{\text{below}}$  values were close to zero (or negative), the median  $\Lambda_{\text{below}}$  was significantly different from zero and also  
 365 positive ( $7.9 \times 10^{-6} \text{ s}^{-1}$ ), with an interquartile range of  $-1.7 \times 10^{-5} \text{ s}^{-1}$  to  $5.3 \times 10^{-5} \text{ s}^{-1}$ . Negative  $\Lambda_{\text{below}}$  values have been reported  
 366 in previous studies (Laakso et al., 2003; Pryor et al., 2016; Zikova and Zdimal, 2016); therefore, we assumed that these negative  
 367 values reflected the uncertainty in measurements and/or inclusion of BC, which might be continuously supplemented in  
 368 airmasses. As the threshold of  $I_{\text{total}}$  increased from 0.01 (all cases) to  $0.2 \text{ mm hr}^{-1}$  (median),  $\Lambda_{\text{below}}$  values were increased by a  
 369 factor of 2.5 to  $2.0 \times 10^{-5} \text{ s}^{-1}$  ( $-2.5 \times 10^{-5} \text{ s}^{-1}$  to  $9.0 \times 10^{-5} \text{ s}^{-1}$ ). Using these obvious increasing tendencies of  $\Lambda_{\text{below}}$  according to  $I_{\text{total}}$ ,  
 370 we determined the empirical fitting equation by investigating the relationship between median  $\Lambda_{\text{below}}$  and each bin of  $I_{\text{total}}$ .  
 371 Figure 5b indicates  $\Lambda_{\text{below}}$  as a function of  $I_{\text{total}}$  based on allocation to 11 logarithmic bins. Because the estimated  $I_{\text{total}}$  bins  
 372 covered the  $I_{\text{total}}$  ranges, 0.03 to  $2.0 \text{ mm hr}^{-1}$  (5<sup>th</sup> percentile to 95<sup>th</sup> percentile), this exponential fitting equation ( $A \times I_{\text{total}}^B$ ) could  
 373 be representative for below-cloud scavenging over East Asia. The constant A and exponent B with a 95% confidence interval  
 374 were  $2.0 \times 10^{-5}$  ( $1.9\text{--}2.2 \times 10^{-5}$ ) and 0.54 (0.46–0.64), respectively. Instead of the SED equation shown in Figure 2, we chose the  
 375 exponential fitting equation because of its higher  $R^2$  (0.973) compared to that from SED fitting (0.903), as well as being widely  
 376 used in previous studies.

377 Figure 6 shows a comparison of  $\Lambda_{\text{below}}$  ~~from reported values~~ calculated using equations from previous studies with ~~this~~  
 378 ~~study that derived using our equation~~ by assuming that the BC size was approximately 200 nm. To compare the measured  $\Lambda_{\text{below}}$ ,  
 379 we used the mean fractional bias (MFB;  $2 \times [A - B] / [A + B]$ ), where A and B denote  ~~$\Lambda_{\text{below}}$  of from calculated reported values~~  
 380 ~~and this study measured  $\Lambda_{\text{below}}$  value~~, respectively. Our newly measured  $\Lambda_{\text{below}}$  values were located in the intermediate range of  
 381 ~~reported-calculated~~  $\Lambda_{\text{below}}$ , and the mean deviations between the measured and all ~~reported-calculated~~ values were relatively  
 382 constant with increasing  $I_{\text{total}}$  because the mean absolute MFBs were slightly increased from 1.4 to 1.6. It should be noted that  
 383  $\Lambda_{\text{below}}$  from Laakso et al. (2003), which is the default scheme for below-cloud scavenging in the FLEXPART model version  
 384 10 or higher (Grythe et al., 2017), showed fairly good agreement with our measured  $\Lambda_{\text{below}}$  among the ~~calculated reported~~  
 385 values (mean absolute MFB of 0.68). MFB was positive at low  $I_{\text{total}}$ , but the opposite tendency was observed for  $I_{\text{total}}$  at  $\sim 0.1$   
 386  $\text{mm hr}^{-1}$ , suggesting that  $\Lambda_{\text{below}}$  might be converged within a similar range when we consider the range of  $I_{\text{total}}$ . Although  
 387 ~~calculated~~  $\Lambda_{\text{below}}$  from Laakso et al. (2003) showed good agreement with our results, the median ~~calculated~~  $\Lambda_{\text{below}}$  ( $6.6 \times 10^{-6} \text{ s}^{-1}$ )  
 388 ~~was overestimated compared to our estimation measured value~~ ( $4.0 \times 10^{-6} \text{ s}^{-1}$ ), by a factor of 1.7 when we recalculated the  
 389 only below-cloud cases. The MFBs from other schemes were too high or low to declare reasonable results. For example, the  
 390  $\Lambda_{\text{below}}$  of secondary ions in Beijing (Xu et al., 2017) had the highest MFB (1.68), and although the diameter ranges were larger

(~ 500 nm) than those of BC, the effect of differences in diameter might be negligible because significant difference in  $\Lambda_{\text{below}}$  between two diameters were not observed (less than 30%) when applied to Laakso et al. (2003).

### 3.5 In-cloud scavenging coefficient ( $\Lambda_{\text{in}}$ )

Compared to  $\Lambda_{\text{below}}$ , the calculation of  $\Lambda_{\text{in}}$  is much more complicated because many factors can influence the in-cloud scavenging process, such as precipitation, total cloud cover (TCC), the specific cloud total water content (CTWC), and so on. A detailed description for the complicated equation for  $\Lambda_{\text{in}}$  in FLEXPART v10 is presented in Grythe et al. (2017), and the equation for  $\Lambda_{\text{in}}$  can be simply expressed as follows:

$$\Lambda_{\text{in}} = \frac{i_{\text{cr}} \cdot F_{\text{nuc}} \cdot I_{\text{total}} \cdot TCC}{CTWC \cdot f_g} \quad (4)$$

where  $i_{\text{cr}}$  and  $F_{\text{nuc}}$  are the cloud water replenishment factor (6.2; default value) and the nucleation efficiency, respectively. It should be mentioned that  $\Lambda_{\text{in}}$  was also calculated by following the FLEXPART scheme using the ERA5 meteorological data (0.25°×0.25°) with HYSPLIT backward trajectory instead of the FLEXPART simulation (1°×1°) to reflect the local variability of meteorological variables ~~match the grid size of the input data with the HYSPLIT backward trajectory~~. Among the 769 cases for in-cloud cases, equations (2) and (3) were also used to calculate TE for only in-cloud cases by substituting  $\Lambda$  with calculated  $\Lambda_{\text{in}}$ . Unlike the hourly measured  $\Lambda_{\text{below}}$  calculated by optimization, the only overall median  $\Lambda_{\text{in}}$  ( $\Lambda_{\text{in}}^*$ ) for in-cloud cases was calculated using equation (3) because  $\Lambda_{\text{in}}$  cannot be constrained by a specific variable.

The ~~FLEXPART-calculated~~  $\Lambda_{\text{in}}^*$  ( $7.28 \times 10^{-6} \text{ s}^{-1}$ ) from FLEXPART scheme (hereafter calculated  $\Lambda_{\text{in}}^*$ ) was underestimated by 1 order of magnitude compared to our ~~estimated-measured~~  $\Lambda_{\text{in}}^*$  ( $8.06 \times 10^{-5} \text{ s}^{-1}$ ). When ~~FLEXPART TE from FLEXPART~~ for in-cloud cases (all cases) was recalculated by considering a ten (five) times higher  $\Lambda_{\text{in}}$ , the median ~~FLEXPART~~ TE was 0.73 (0.79), which was much close to the measured TE (both 0.72). Although the grid size of input meteorological data for two approaches did not match, the underestimation of the in-cloud scavenging scheme in FLEXPART was confirmed. Grythe et al. (2017) reported an overestimation of observed BC (a factor of 1.68) due to inaccurate emission sources rather than the underestimated in-cloud removal efficiencies. Although the effect of BC particle dispersion to adjacent grid cells was neglected in our approach, the underestimation of in-cloud scavenging coefficients was obvious because the accuracy of the emission inventory did not affect the ~~estimated-measured~~  $\Lambda_{\text{in}}^*$ . Looking more closely into the sites, the ~~calculated FLEXPART~~  $\Lambda_{\text{in}}^*$  at Noto was remarkably underestimated by 1 order of magnitude, followed by Gosan (~90%) and Baengnyeong (~43%), similar to the order of the wet removal efficiency. It should be noted that the coefficient of variation (CV; standard deviation divided by the mean) of ~~calculated FLEXPART~~  $\Lambda_{\text{in}}^*$  was much lower (0.23) than the measured  $\Lambda_{\text{in}}^*$  (0.78), indicating that ~~calculated FLEXPART~~  $\Lambda_{\text{in}}^*$  did not accurately represent the actual regional difference in the real world. Among the input meteorological variables in equation (4), the CV of  $I_{\text{total}}$  was the highest as 0.22, which was similar to the CV of ~~calculated FLEXPART~~  $\Lambda_{\text{in}}^*$ , followed by CTWC (0.08),  $f_g$  (0.03), and TCC (0.02), suggesting that the difference in ~~calculated FLEXPART~~  $\Lambda_{\text{in}}^*$  could be partially explained by  $I_{\text{total}}$  rather than other variables. Among the meteorological variables that were not considered in equation (4), the convective available potential energy (CAPE), which is well known as an indicator of vertical instability (Mori et al., 2014), had the highest CV of 0.31.

We employed an artificial neural network (ANN) to compare the importance of CAPE with other considered input meteorological variables for determining the hourly  $\Lambda_{\text{in}}$ , not  $\Lambda_{\text{in}}^*$ . We applied a stricter selection for in-cloud cases, i.e., only when in-cloud scavenging occurred less than three times (i.e., three cells) in a single case, regardless of the number of below-cloud occurrences. Because the effect of below-cloud scavenging was successfully excluded from the TE using the derived

428 equation for  $\Lambda_{\text{below}}$  in the previous section, the  $\Lambda_{\text{in}}$  in less than three in-cloud cases can also be calculated by optimization based  
429 on the remaining TE. We applied a threshold of three cases here because the number of data (230 cases) was sufficient to  
430 conduct statistical analysis, while the optimization uncertainty could be reduced to its minimum. The ANN model was trained  
431 using six meteorological variables (CAPE, CTWC,  $f_g$ ,  $F_{\text{nuc}}$ ,  $I_{\text{total}}$ , and TCC), and all variables were normalized by the minimum  
432 and maximum of each variable ( $[x - \min(x)] / [\max(x) - \min(x)]$ ). To determine the optimal node numbers in the hidden layer, we  
433 applied the ‘caret’ package of the R function that contains several sets of machine learning modes and validation tools  
434 (<https://cran.r-project.org/web/packages/caret/caret.pdf>) and adopted a method from the ‘neuralnet’ package that is fit for a  
435 multi-hidden layer. By varying the ‘size’ (node number) from 5 to 20 and using  $k$ -fold cross validation, the selected cases were  
436 randomly divided by a ratio of 3:1 into training (172 data points) and validation data (58 data points). Garson’s algorithm in  
437 the “NeuralNetTools” package was used to identify the relative importance of six input variables in the final neural network  
438 (Garson, 1991). The model’s performance was assessed in these independent validation data by calculating the root mean  
439 squared error. The optimal number of nodes in the hidden layer was 12 (Figure 7a).

440 Figure 7b shows the relative importance of input variables for calculating  $\Lambda_{\text{in}}$  using Garson’s algorithm. The most important  
441 input variable was CAPE, with a value of 35%, followed by CTWC,  $I_{\text{total}}$ , and so on, thus confirming that CAPE should be  
442 considered in the  $\Lambda_{\text{in}}$  calculation. Typically, enhancing wet removal by convective clouds successfully reduces the aloft BC  
443 concentration in the free troposphere (Koch et al., 2009). Therefore, convective process is important in tropical regions but has  
444 a slightly lower impact at mid-latitudes (Luo et al., 2019; Grythe et al., 2017; Xu et al., 2019). Moreover, previous studies have  
445 highlighted convective scavenging to be a key parameter in determining the BC concentration in model simulations (Lund et  
446 al., 2017; Xu et al., 2019) and the role of wet removal by convective clouds might be significant when most airmasses travel  
447 above the planetary boundary layer. Unfortunately, the current version of FLEXPART does not implement convective  
448 scavenging (Philipp and Seibert, 2018), which could be a plausible reason for the underestimation of calculated FLEXPART  
449  $\Lambda_{\text{in}}$ . Although the relative importance of each variable cannot be parameterized to calculate  $\Lambda_{\text{in}}$ , this approach highlights that  
450 CAPE is one of the key factors for determining  $\Lambda_{\text{in}}$  over East Asia. In the future, more information might be required to evaluate  
451 the in-cloud scavenging scheme using Weather Research and Forecasting (WRF)-FLEXPART at a higher resolution in further  
452 studies since a 0.25° grid size is still not sufficient to reproduce convective clouds (typically 10 km or less).

#### 453 4 Conclusions

454 The wet removal rates and scavenging coefficients for BC were investigated by the term of  $\Delta\text{BC}/\Delta\text{CO}$  ratios from long-  
455 term, best-effort observations at three remote sites in East Asia (Baengnyeong and Gosan in South Korea and Noto in Japan).  
456 By combining the backward trajectories covering the past 72 h, the accumulated precipitation along trajectories (APT), and  
457 transport efficiency (TE;  $[\Delta\text{BC}/\Delta\text{CO}]_{\text{APT}>0} / [\Delta\text{BC}/\Delta\text{CO}]_{\text{APT}=0}$ ), BC wet removal efficiency was assessed as an aspect of the  
458 pathway of trajectories, including the successful identification of below- and in-cloud cases. The overall wet removal rates as  
459 a function of APT, the half-life and  $e$ -folding lifetime were similar to those of previous studies but showed large regional  
460 differences depending on the measurement site. The difference in the wet removal rate, depending on the measurement site,  
461 can be explained by the different meteorological conditions, such as the precipitation rate, cloud cover, total column cloud  
462 water, and cloud bottom height. The differences in regional and seasonal wet removal rates ~~could be explained~~ might be  
463 influenced by the frequency of exposure to below- and in-cloud scavenging condition during transport as well as the magnitude  
464 of aging process causing the different coating thicknesses ~~the different coating thicknesses according to the BC emission~~  
465 ~~sources (thin and thick coated BC from the industrial and residential sectors, respectively)~~ because the thick-coated BC  
466 particles are preferentially removed due to cloud processes. By discriminating below- and in-cloud dominant cases according

467 to cloud vertical information from ERA5 pressure level data, scavenging coefficients for below-cloud ( $\Lambda_{\text{below}}$ ) and in-cloud  
468 ( $\Lambda_{\text{in}}^*$ ) were simply converted from the measured TE values. The calculated  $\Lambda_{\text{below}}$  from the FLEXPART scheme was  
469 overestimated by a factor of 1.7 compared to the measured  $\Lambda_{\text{below}}$ , although the measured  $\Lambda_{\text{below}}$  showed good agreement with  
470 the below-cloud scheme in FLEXPART among the reported scavenging coefficients. In contrast to  $\Lambda_{\text{below}}$ , the  
471 calculated FLEXPART  $\Lambda_{\text{in}}^*$  from FLEXPART scheme was highly underestimated by 1 order of magnitude compared to  
472 measured  $\Lambda_{\text{in}}^*$ , suggesting that the current in-cloud scavenging scheme did not represent regional variability. By diagnosing  
473 the relative importance of the input variables using the artificial neuron network (ANN), we found that the convective available  
474 potential energy (CAPE), which is an indicator of vertical instability, should be considered to improve the in-cloud scavenging  
475 scheme because convective scavenging could be regarded as a key parameter for determining the accurate BC concentration  
476 in a model. This study could contribute not only to improving the below-cloud scavenging scheme implemented in a model,  
477 especially FLEXPART, but also to providing evidence for complementary in-cloud scavenging schemes by considering the  
478 convective scavenging process. For the first time, these results suggest a novel and straightforward approach to evaluating the  
479 wet scavenging scheme in various models and to enhancing the understanding of BC behavior by excluding the effects of  
480 inaccurate emission inventories.

#### 481 **Author contributions.**

482 YC and YK designed the study and prepared the paper, with contributions from all co-authors. YC, MT, and CZ optimized  
483 the FLEXPART model and revised the paper. YC conducted the FLEXPART model simulations and performed the analyses.  
484 SMP was responsible for measurements at Baengnyeong. AM and YS conducted measurements at Noto, and SWK contributed  
485 to ground observations and quality control at Gosan. XP and IP contributed to the data analysis. All co-authors provided  
486 professional comments to improve the paper.

#### 487 **Competing interests.**

488 The authors declare that they have no conflicts of interest.

#### 489 **Code/Data availability.**

490 The observational data set for BC and CO are available upon request to the corresponding author.

#### 491 **Acknowledgments.**

492 The authors thank NOAA ARL and ECMWF for providing the HYSPLIT model and ERA5 meteorological data. We also  
493 thank anonymous reviewers for precise and valuable comments that greatly improved the manuscript.

#### 494 **Financial support.**

495 This research has been supported by the Environment Research and Technology Development Fund of the Ministry of the  
496 Environment, Japan (grant no. 2-1803).



## References

- Andronache, C.: Estimated variability of below-cloud aerosol removal by rainfall for observed aerosol size distributions, *Atmos. Chem. Phys.*, 3, 131-143, 10.5194/acp-3-131-2003, 2003.
- Ashbaugh, L. L., Malm, W. C., and Sadeh, W. Z.: A residence time probability analysis of sulfur concentrations at grand Canyon National Park, *Atmos. Environ.*, 19, 1263-1270, [https://doi.org/10.1016/0004-6981\(85\)90256-2](https://doi.org/10.1016/0004-6981(85)90256-2), 1985.
- Baklanov, A., and Sørensen, J. H.: Parameterisation of radionuclide deposition in atmospheric long-range transport modelling, *Physics and Chemistry of the Earth, Part B: Hydrology, Oceans and Atmosphere*, 26, 787-799, [https://doi.org/10.1016/S1464-1909\(01\)00087-9](https://doi.org/10.1016/S1464-1909(01)00087-9), 2001.
- Bond, T. C., Anderson, T. L., and Campbell, D.: Calibration and Intercomparison of Filter-Based Measurements of Visible Light Absorption by Aerosols, *Aerosol Sci. Technol.*, 30, 582–600, <https://doi.org/10.1080/027868299304435>, 1999.
- Bond, T. C., Doherty, S. J., Fahey, D., Forster, P., Berntsen, T., DeAngelo, B., Flanner, M., Ghan, S., Kärcher, B., and Koch, D.: Bounding the role of black carbon in the climate system: A scientific assessment, *J. Geophys. Res. Atmos.*, 118, 5380-5552, 2013.
- Choi, Y., Kanaya, Y., Park, S. M., Matsuki, A., Sadanaga, Y., Kim, S. W., Uno, I., Pan, X., Lee, M., Kim, H., and Jung, D. H.: Regional variability in black carbon and carbon monoxide ratio from long-term observations over East Asia: assessment of representativeness for black carbon (BC) and carbon monoxide (CO) emission inventories, *Atmos. Chem. Phys.*, 20, 83-98, 10.5194/acp-20-83-2020, 2020.
- Chung, S. H., and Seinfeld, J. H.: Global distribution and climate forcing of carbonaceous aerosols, *Journal of Geophysical Research: Atmospheres*, 107, AAC 14-11-AAC 14-33, 10.1029/2001jd001397, 2002.
- Cooke, W. F., and Wilson, J. J. N.: A global black carbon aerosol model, *Journal of Geophysical Research: Atmospheres*, 101, 19395-19409, 10.1029/96jd00671, 1996.
- Crippa, M., Guizzardi, D., Muntean, M., Schaaf, E., Dentener, F., van Aardenne, J. A., Monni, S., Doering, U., Olivier, J. G. J., Pagliari, V., and Janssens-Maenhout, G.: Gridded emissions of air pollutants for the period 1970–2012 within EDGAR v4.3.2, *Earth Syst. Sci. Data*, 10, 1987–2013, 10.5194/essd-10-1987-2018, 2018.
- Croft, B., Lohmann, U., Martin, R. V., Stier, P., Wurzler, S., Feichter, J., Hoose, C., Heikkilä, U., van Donkelaar, A., and Ferrachat, S.: Influences of in-cloud aerosol scavenging parameterizations on aerosol concentrations and wet deposition in ECHAM5-HAM, *Atmos. Chem. Phys.*, 10, 1511-1543, 10.5194/acp-10-1511-2010, 2010.
- Draxler, R., Stunder, B., Rolph, G., Stein, A., and Taylor, A.: HYSPLIT4 User's Guide Version 4-Last Revision: February 2018, HYSPLIT Air Resources Laboratory, MD, USA, 2018.
- Ding, S., Zhao, D., He, C., Huang, M., He, H., Tian, P., Liu, Q., Bi, K., Yu, C., Pitt, J., Chen, Y., Ma, X., Chen, Y., Jia, X., Kong, S., Wu, J., Hu, D., Hu, K., Ding, D., and Liu, D.: Observed Interactions Between Black Carbon and Hydrometeor During Wet Scavenging in Mixed-Phase Clouds, *Geophysical Research Letters*, 46, 8453-8463, 10.1029/2019gl083171, 2019.
- Eck, T. F., Holben, B. N., Reid, J. S., Xian, P., Giles, D. M., Sinyuk, A., Smirnov, A., Schafer, J. S., Slutsker, I., Kim, J., Koo, J. H., Choi, M., Kim, K. C., Sano, I., Arola, A., Sayer, A. M., Levy, R. C., Munchak, L. A., O'Neill, N. T., Lyapustin, A., Hsu, N. C., Randles, C. A., Da Silva, A. M., Buchar, V., Govindaraju, R. C., Hyer, E., Crawford, J. H., Wang, P., and Xia, X.: Observations of the Interaction and Transport of Fine Mode Aerosols With Cloud and/or Fog in Northeast Asia From Aerosol Robotic Network and Satellite Remote Sensing, *Journal of Geophysical Research: Atmospheres*, 0, 10.1029/2018JD028313, 2018.
- Emmons, L. K., Walters, S., Hess, P. G., Lamarque, J. F., Pfister, G. G., Fillmore, D., Granier, C., Guenther, A., Kinnison, D., Laepple, T., Orlando, J., Tie, X., Tyndall, G., Wiedinmyer, C., Baughcum, S. L., and Kloster, S.: Description and evaluation of the Model for Ozone and Related chemical Tracers, version 4 (MOZART-4), *Geosci. Model Dev.*, 3, 43-67, 10.5194/gmd-3-43-2010, 2010.
- Emerson, E. W., Katich, J. M., Schwarz, J. P., McMeeking, G. R., and Farmer, D. K.: Direct Measurements of Dry and Wet Deposition of Black Carbon Over a Grassland, *J. Geophys. Res. Atmos.*, 123, 12,277-212,290, 10.1029/2018JD028954, 2018.
- Feng, J.: A 3-mode parameterization of below-cloud scavenging of aerosols for use in atmospheric dispersion models, *Atmos. Environ.*, 41, 6808-6822, <https://doi.org/10.1016/j.atmosenv.2007.04.046>, 2007.
- Garson, G. D.: Interpreting neural-network connection weights, *Artif. Intell. Expert*, 6, 46–51, 1991.
- Grythe, H., Kristiansen, N. I., Groot Zwaafink, C. D., Eckhardt, S., Ström, J., Tunved, P., Krejci, R., and Stohl, A.: A new aerosol wet removal scheme for the Lagrangian particle model FLEXPART v10, *Geosci. Model Dev.*, 10, 1447-1466, 10.5194/gmd-10-1447-2017, 2017.
- Guo, Q., Hu, M., Guo, S., Wu, Z., Peng, J., and Wu, Y.: The variability in the relationship between black carbon and carbon monoxide over the eastern coast of China: BC aging during transport, *Atmos. Chem. Phys.*, 17, 10395–10403, <https://doi.org/10.5194/acp-17-10395-2017>, 2017.
- Han, C., Li, S. M., Liu, P., and Lee, P.: Size Dependence of the Physical Characteristics of Particles Containing Refractory Black Carbon in Diesel Vehicle Exhaust, *Environmental Science & Technology*, 53, 137–145, 10.1021/acs.est.8b04603,

- [2019-Hoffmann, L., Günther, G., Li, D., Stein, O., Wu, X., Griessbach, S., Heng, Y., Konopka, P., Müller, R., Vogel, B., and Wright, J. S.: From ERA-Interim to ERA5: the considerable impact of ECMWF's next-generation reanalysis on Lagrangian transport simulations, \*Atmos. Chem. Phys.\*, \*\*19\*\*, 3097–3124, <https://doi.org/10.5194/acp-19-3097-2019>, 2019.](#)
- Jylhä, K.: Empirical scavenging coefficients of radioactive substances released from chernobyl, *Atmospheric Environment. Part A. General Topics*, **25**, 263-270, [https://doi.org/10.1016/0960-1686\(91\)90297-K](https://doi.org/10.1016/0960-1686(91)90297-K), 1991.
- [Kanaya, Y., Komazaki, Y., Pochanart, P., Liu, Y., Akimoto, H., Gao, J., Wang, T., and Wang, Z.: Mass concentrations of black carbon measured by four instruments in the middle of Central East China in June 2006, \*Atmos. Chem. Phys.\*, \*\*8\*\*, 7637–7649, <https://doi.org/10.5194/acp-8-7637-2008>, 2008.](#)
- Kanaya, Y., Taketani, F., Komazaki, Y., Liu, X., Kondo, Y., Sahu, L. K., Irie, H., and Takashima, H.: Comparison of Black Carbon Mass Concentrations Observed by Multi-Angle Absorption Photometer (MAAP) and Continuous Soot-Monitoring System (COSMOS) on Fukue Island and in Tokyo, Japan, *Aerosol Sci. Technol.*, **47**, 1-10, 10.1080/02786826.2012.716551, 2013.
- Kanaya, Y., Pan, X., Miyakawa, T., Komazaki, Y., Taketani, F., Uno, I., and Kondo, Y.: Long-term observations of black carbon mass concentrations at Fukue Island, western Japan, during 2009–2015: constraining wet removal rates and emission strengths from East Asia, *Atmos. Chem. Phys.*, **16**, 10689-10705, 10.5194/acp-16-10689-2016, 2016.
- Kanaya, Y., Yamaji, K., Miyakawa, T., Taketani, F., Zhu, C., Choi, Y., Komazaki, Y., Ikeda, K., Kondo, Y., and Klimont, Z.: Rapid reduction of black carbon emissions from China: evidence from 2009-2019 observations on Fukue Island, Japan, *Atmos. Chem. Phys.*, **20**, 6339–6356, <https://doi.org/10.5194/acp-20-6339-2020>, 2020. *Atmos. Chem. Phys. Discuss.*, **2019**, 1–28, 10.5194/acp-2019-1054, 2019.–
- [Koch, D., and Hansen, J.: Distant origins of Arctic black carbon: A Goddard Institute for Space Studies ModelE experiment, \*Journal of Geophysical Research: Atmospheres\*, \*\*110\*\*, 10.1029/2004jd005296, 2005.](#)
- Koch, D., Schulz, M., Kinne, S., McNaughton, C., Spackman, J. R., Balkanski, Y., Bauer, S., Berntsen, T., Bond, T. C., Boucher, O., Chin, M., Clarke, A., De Luca, N., Dentener, F., Diehl, T., Dubovik, O., Easter, R., Fahey, D. W., Feichter, J., Fillmore, D., Freitag, S., Ghan, S., Ginoux, P., Gong, S., Horowitz, L., Iversen, T., Kirkev, aring, g, A., Klimont, Z., Kondo, Y., Krol, M., Liu, X., Miller, R., Montanaro, V., Moteki, N., Myhre, G., Penner, J. E., Perlwitz, J., Pitari, G., Reddy, S., Sahu, L., Sakamoto, H., Schuster, G., Schwarz, J. P., Seland, Ø., Stier, P., Takegawa, N., Takemura, T., Textor, C., van Aardenne, J. A., and Zhao, Y.: Evaluation of black carbon estimations in global aerosol models, *Atmos. Chem. Phys.*, **9**, 9001-9026, 10.5194/acp-9-9001-2009, 2009.
- Kondo, Y., Moteki, N., Oshima, N., Ohata, S., Koike, M., Shibano, Y., Takegawa, N., and Kita, K.: Effects of wet deposition on the abundance and size distribution of black carbon in East Asia, *J. Geophys. Res. Atmos.*, **121**, 4691-4712, 10.1002/2015JD024479, 2016.
- Kurokawa, J., Ohara, T., Morikawa, T., Hanayama, S., Janssens-Maenhout, G., Fukui, T., Kawashima, K., and Akimoto, H.: Emissions of air pollutants and greenhouse gases over Asian regions during 2000–2008: Regional Emission inventory in ASia (REAS) version 2, *Atmos. Chem. Phys.*, **13**, 11019-11058, 10.5194/acp-13-11019-2013, 2013.
- Kuwata, M., Kondo, Y., Mochida, M., Takegawa, N., and Kawamura, K.: Dependence of CCN activity of less volatile particles on the amount of coating observed in Tokyo, *Journal of Geophysical Research: Atmospheres*, **112**, 10.1029/2006jd007758, 2007.
- Laakso, L., Grönholm, T., Rannik, Ü., Kosmale, M., Fiedler, V., Vehkamäki, H., and Kulmala, M.: Ultrafine particle scavenging coefficients calculated from 6 years field measurements, *Atmos. Environ.*, **37**, 3605-3613, [https://doi.org/10.1016/S1352-2310\(03\)00326-1](https://doi.org/10.1016/S1352-2310(03)00326-1), 2003.
- Lamb, K. D., Perring, A. E., Samset, B., Peterson, D., Davis, S., Anderson, B. E., Beyersdorf, A., Blake, D. R., Campuzano-Jost, P., Corr, C. A., Diskin, G. S., Kondo, Y., Moteki, N., Nault, B. A., Oh, J., Park, M., Pusede, S. E., Simpson, I. J., Thornhill, K. L., Wisthaler, A., and Schwarz, J. P.: Estimating Source Region Influences on Black Carbon Abundance, Microphysics, and Radiative Effect Observed Over South Korea, *J. Geophys. Res. Atmos.*, **123**, 13,527-513,548, doi:10.1029/2018JD029257, 2018.
- Lee, Y. H., Lamarque, J. F., Flanner, M. G., Jiao, C., Shindell, D. T., Berntsen, T., Bisiaux, M. M., Cao, J., Collins, W. J., Curran, M., Edwards, R., Faluvegi, G., Ghan, S., Horowitz, L. W., McConnell, J. R., Ming, J., Myhre, G., Nagashima, T., Naik, V., Rumbold, S. T., Skeie, R. B., Sudo, K., Takemura, T., Thevenon, F., Xu, B., and Yoon, J. H.: Evaluation of preindustrial to present-day black carbon and its albedo forcing from Atmospheric Chemistry and Climate Model Intercomparison Project (ACCMIP), *Atmos. Chem. Phys.*, **13**, 2607-2634, 10.5194/acp-13-2607-2013, 2013.
- [Li, M., Zhang, Q., Kurokawa, J. I., Woo, J. H., He, K., Lu, Z., Ohara, T., Song, Y., Streets, D. G., Carmichael, G. R., Cheng, Y., Hong, C., Huo, H., Jiang, X., Kang, S., Liu, F., Su, H., and Zheng, B.: MIX: a mosaic Asian anthropogenic emission inventory under the international collaboration framework of the MICS-Asia and HTAP, \*Atmos. Chem. Phys.\*, \*\*17\*\*, 935–963, 10.5194/acp-17-935-2017, 2017.](#)
- Li, S., Park, S., Park, M.-K., Jo, C. O., Kim, J.-Y., Kim, J.-Y., and Kim, K.-R.: Statistical Back Trajectory Analysis for Estimation of CO2 Emission Source Regions, *Atmosphere*, **24**, 245-251, 2014 (Abstract in English).
- [Liu, D., Joshi, R., Wang, J., Yu, C., Allan, J. D., Coe, H., Flynn, M. J., Xie, C., Lee, J., Squires, F., Kotthaus, S., Grimmond, S., Ge, X., Sun, Y., and Fu, P.: Contrasting physical properties of black carbon in urban Beijing between winter and summer, \*Atmos. Chem. Phys.\*, \*\*19\*\*, 6749–6769, 10.5194/acp-19-6749-2019, 2019.](#)
- Liu, L., Zhang, J., Xu, L., Yuan, Q., Huang, D., Chen, J., Shi, Z., Sun, Y., Fu, P., Wang, Z., Zhang, D., and Li, W.: Cloud scavenging of anthropogenic refractory particles at a mountain site in North China, *Atmos. Chem. Phys.*, **18**, 14681-14693,

- 10.5194/acp-18-14681-2018, 2018.
- Lund, M. T., Berntsen, T. K., and Samset, B. H.: Sensitivity of black carbon concentrations and climate impact to aging and scavenging in OsloCTM2–M7, *Atmos. Chem. Phys.*, 17, 6003–6022, 10.5194/acp-17-6003-2017, 2017.
- Lund, M. T., Samset, B. H., Skeie, R. B., Watson-Parris, D., Katich, J. M., Schwarz, J. P., and Weinzierl, B.: Short Black Carbon lifetime inferred from a global set of aircraft observations, *npj Climate and Atmospheric Science*, 1, 31, 10.1038/s41612-018-0040-x, 2018.
- Luo, G., Yu, F., and Schwab, J.: Revised treatment of wet scavenging processes dramatically improves GEOS-Chem 12.0.0 simulations of surface nitric acid, nitrate, and ammonium over the United States, *Geosci. Model Dev.*, 12, 3439–3447, 10.5194/gmd-12-3439-2019, 2019.
- Matsui, H., Koike, M., Kondo, Y., Moteki, N., Fast, J. D., and Zaveri, R. A.: Development and validation of a black carbon mixing state resolved three-dimensional model: Aging processes and radiative impact, *J. Geophys. Res. Atmos.*, 118, 2304–2326, 10.1029/2012jd018446, 2013.
- Matsui, H., Hamilton, D. S., and Mahowald, N. M.: Black carbon radiative effects highly sensitive to emitted particle size when resolving mixing-state diversity, *Nature Communications*, 9, 3446, 10.1038/s41467-018-05635-1, 2018.
- Miyakawa, T., Kanaya, Y., Komazaki, Y., Taketani, F., Pan, X., Irwin, M., and Symonds, J.: Intercomparison between a single particle soot photometer and evolved gas analysis in an industrial area in Japan: Implications for the consistency of soot aerosol mass concentration measurements, *Atmos. Environ.*, 127, 14–21, <https://doi.org/10.1016/j.atmosenv.2015.12.018>, 2016.
- Miyakawa, T., Oshima, N., Taketani, F., Komazaki, Y., Yoshino, A., Takami, A., Kondo, Y., and Kanaya, Y.: Alteration of the size distributions and mixing states of black carbon through transport in the boundary layer in east Asia, *Atmos. Chem. Phys.*, 17, 5851–5864, 10.5194/acp-17-5851-2017, 2017.
- Mori, T., Kondo, Y., Ohata, S., Moteki, N., Matsui, H., Oshima, N., and Iwasaki, A.: Wet deposition of black carbon at a remote site in the East China Sea, *J. Geophys. Res. Atmos.*, 119, 10485–10498, 10.1002/2014jd022103, 2014.
- Moteki, N., Kondo, Y., Miyazaki, Y., Takegawa, N., Komazaki, Y., Kurata, G., Shirai, T., Blake, D. R., Miyakawa, T., and Koike, M.: Evolution of mixing state of black carbon particles: Aircraft measurements over the western Pacific in March 2004, *Geophysical Research Letters*, 34, 10.1029/2006gl028943, 2007.
- Moteki, N., Kondo, Y., Oshima, N., Takegawa, N., Koike, M., Kita, K., Matsui, H., and Kajino, M.: Size dependence of wet removal of black carbon aerosols during transport from the boundary layer to the free troposphere, *Geophysical Research Letters*, 39, 10.1029/2012gl02034, 2012.
- Myhre, G., Shindell, D., Bréon, F.-M., Collins, W., Fuglestad, J., Huang, J., Koch, D., Lamarque, J.-F., Lee, D., and Mendoza, B. J. C. c.: Anthropogenic and natural radiative forcing, 423, 658–740, 2013.
- Ogren, J. A., Wendell, J., Andrews, E., and Sheridan, P. J.: Continuous light absorption photometer for long-term studies, *Atmos. Meas. Tech.*, 10, 4805–4818, 10.5194/amt-10-4805-2017, 2017.
- Oh, J., Park, J.-S., Ahn, J.-Y., Choi, J.-S., Lim, J.-H., Kim, H.-J., Han, J.-S., Hong, Y.-D., and Lee, G.-W.: A study on the Behavior of the Black Carbon at Baengnyeong Island of Korea Peninsular, *J. Korean Soc. Urban Environ.*, 14, 67–76, 2014 (Abstract in English).
- Oh, J., Park, J., Lee, S., Ahn, J., Choi, J., Lee, S., Lee, Y., Kim, H., Hong, Y., Hong, J., Kim, J., Kim, S., and Lee, G.-W.: Characteristics of Black Carbon Particles in Ambient Air Using a Single Particle Soot Photometer (SP2) in May 2013, Jeju, Korea, *J. Korean Soc. Atmos.*, 32, 255–268, 2015 (Abstract in English).
- Ohata, S., Kondo, Y., Moteki, N., Mori, T., Yoshida, A., Sinha, P. R., and Koike, M.: Accuracy of black carbon measurements by a filter-based absorption photometer with a heated inlet, *Aerosol Science and Technology*, 53, 1079–1091, 10.1080/02786826.2019.1627283, 2019.
- Oshima, N., Kondo, Y., Moteki, N., Takegawa, N., Koike, M., Kita, K., Matsui, H., Kajino, M., Nakamura, H., Jung, J. S., and Kim, Y. J.: Wet removal of black carbon in Asian outflow: Aerosol Radiative Forcing in East Asia (A-FORCE) aircraft campaign, *J. Geophys. Res. Atmos.*, 117, 10.1029/2011JD016552, 2012.
- Park, J., Song, I., Kim, H., Lim, H., Park, S., Shin, S., Shin, H., Lee, S., and Kim, J.: The Characteristics of Black Carbon of Seoul, *J. Environ. Impact Assess.*, 28, 113–128, 10.14249/EIA.2019.28.2.113, 2019 (Abstract in English).
- Park, R. J., Jacob, D. J., Palmer, P. I., Clarke, A. D., Weber, R. J., Zondlo, M. A., Eisele, F. L., Bandy, A. R., Thornton, D. C., Sachse, G. W., and Bond, T. C.: Export efficiency of black carbon aerosol in continental outflow: Global implications, *J. Geophys. Res.-Atmos.*, 110, 1–7, <https://doi.org/10.1029/2004JD005432>, 2005.
- Philipp, A., and Seibert, P.: Scavenging and Convective Clouds in the Lagrangian Dispersion Model FLEXPART, in: *Air Pollution Modeling and its Application XXV*, Cham, 2018, 335–340.
- Pisso, I., Sollum, E., Grythe, H., Kristiansen, N. I., Cassiani, M., Eckhardt, S., Arnold, D., Morton, D., Thompson, R. L., Groot Zwaaftink, C. D., Evangelou, N., Sodemann, H., Haimberger, L., Henne, S., Brunner, D., Burkhart, J. F., Fouilloux, A., Brioude, J., Philipp, A., Seibert, P., and Stohl, A.: The Lagrangian particle dispersion model FLEXPART version 10.4, *Geosci. Model Dev.*, 12, 4955–4997, 10.5194/gmd-12-4955-2019, 2019.
- Pryor, S. C., Joerger, V. M., and Sullivan, R. C.: Empirical estimates of size-resolved precipitation scavenging coefficients for ultrafine particles, *Atmos. Environ.*, 143, 133–138, <https://doi.org/10.1016/j.atmosenv.2016.08.036>, 2016.
- Samset, B. H., Myhre, G., Herber, A., Kondo, Y., Li, S. M., Moteki, N., Koike, M., Oshima, N., Schwarz, J. P., Balkanski, Y., Bauer, S. E., Bellouin, N., Berntsen, T. K., Bian, H., Chin, M., Diehl, T., Easter, R. C., Ghan, S. J., Iversen, T., Kirkevåg, A., Lamarque, J. F., Lin, G., Liu, X., Penner, J. E., Schulz, M., Seland, Ø., Skeie, R. B., Stier, P., Takemura, T., Tsigaridis,

- K., and Zhang, K.: Modelled black carbon radiative forcing and atmospheric lifetime in AeroCom Phase II constrained by aircraft observations, *Atmos. Chem. Phys.*, 14, 12465-12477, 10.5194/acp-14-12465-2014, 2014.
- [Schwarz, J. P., Spackman, J. R., Gao, R. S., Watts, L. A., Stier, P., Schulz, M., Davis, S. M., Wofsy, S. C., and Fahey, D. W.: Global-scale black carbon profiles observed in the remote atmosphere and compared to models, \*Geophysical Research Letters\*, 37, 10.1029/2010gl044372, 2010.](#)
- [Sharma, S., Ishizawa, M., Chan, D., Lavoué, D., Andrews, E., Eleftheriadis, K., and Maksyutov, S.: 16-year simulation of Arctic black carbon: Transport, source contribution, and sensitivity analysis on deposition, \*Journal of Geophysical Research: Atmospheres\*, 118, 943-964, 10.1029/2012jd017774, 2013.](#)
- Sparmacher, H., Fülber, K., and Bonka, H.: Below-cloud scavenging of aerosol particles: Particle-bound radionuclides—Experimental, *Atmospheric Environment. Part A. General Topics*, 27, 605-618, [https://doi.org/10.1016/0960-1686\(93\)90218-N](https://doi.org/10.1016/0960-1686(93)90218-N), 1993.
- [Stier, P., Seinfeld, J. H., Kinne, S., and Boucher, O.: Aerosol absorption and radiative forcing, \*Atmos. Chem. Phys.\*, 7, 5237-5261, 10.5194/acp-7-5237-2007, 2007.](#)
- Stohl, A., Forster, C., Frank, A., Seibert, P., and Wotawa, G.: Technical note: The Lagrangian particle dispersion model FLEXPART version 6.2, *Atmos. Chem. Phys.*, 5, 2461-2474, 10.5194/acp-5-2461-2005, 2005.
- [Taketani, F., Kanaya, Y., Nakayama, T., Ueda, S., Matsumi, Y., Sadanaga, Y., Iwamoto, Y., and Matsuki, A.: Property of Black Carbon Particles Measured by a Laser-Induced Incandescence Technique in the spring at Noto Peninsula, Japan, \*J. Aerosol Res.\*, 31, 194-202, <https://doi.org/10.11203/jar.31.194>, 2016 \(Abstract in English\).](#)
- Textor, C., Schulz, M., Guibert, S., Kinne, S., Balkanski, Y., Bauer, S., Bernsten, T., Berglen, T., Boucher, O., Chin, M., Dentener, F., Diehl, T., Easter, R., Feichter, H., Fillmore, D., Ghan, S., Ginoux, P., Gong, S., Grini, A., Hendricks, J., Horowitz, L., Huang, P., Isaksen, I., Iversen, I., Kloster, S., Koch, D., Kirkevåg, A., Kristjansson, J. E., Krol, M., Lauer, A., Lamarque, J. F., Liu, X., Montanaro, V., Myhre, G., Penner, J., Pitari, G., Reddy, S., Seland, Ø., Stier, P., Takemura, T., and Tie, X.: Analysis and quantification of the diversities of aerosol life cycles within AeroCom, *Atmos. Chem. Phys.*, 6, 1777-1813, 10.5194/acp-6-1777-2006, 2006.
- Ueda, S., Nakayama, T., Taketani, F., Adachi, K., Matsuki, A., Iwamoto, Y., Sadanaga, Y., and Matsumi, Y.: Light absorption and morphological properties of soot-containing aerosols observed at an East Asian outflow site, Noto Peninsula, Japan, *Atmos. Chem. Phys.*, 16, 2525-2541, 10.5194/acp-16-2525-2016, 2016.
- [Vignati, E., Karl, M., Krol, M., Wilson, J., Stier, P., and Cavalli, F.: Sources of uncertainties in modelling black carbon at the global scale, \*Atmos. Chem. Phys.\*, 10, 2595-2611, 10.5194/acp-10-2595-2010, 2010.](#)
- Wang, Q., Jacob, D. J., Spackman, J. R., Perring, A. E., Schwarz, J. P., Moteki, N., Marais, E. A., Ge, C., Wang, J., and Barrett, S. R. H.: Global budget and radiative forcing of black carbon aerosol: Constraints from pole-to-pole (HIPPO) observations across the Pacific, *Journal of Geophysical Research: Atmospheres*, 119, 195-206, 10.1002/2013jd020824, 2014a.
- Wang, X., Zhang, L., and Moran, M. D.: Development of a new semi-empirical parameterization for below-cloud scavenging of size-resolved aerosol particles by both rain and snow, *Geosci. Model Dev.*, 7, 799-819, 10.5194/gmd-7-799-2014, 2014b.
- Winiger, P., Andersson, A., Eckhardt, S., Stohl, A., and Gustafsson, Ö.: The sources of atmospheric black carbon at a European gateway to the Arctic, *Nature Communications*, 7, 12776, 10.1038/ncomms12776, 2016.
- Xu, D., Ge, B., Wang, Z., Sun, Y., Chen, Y., Ji, D., Yang, T., Ma, Z., Cheng, N., Hao, J., and Yao, X.: Below-cloud wet scavenging of soluble inorganic ions by rain in Beijing during the summer of 2014, *Environmental Pollution*, 230, 963-973, <https://doi.org/10.1016/j.envpol.2017.07.033>, 2017.
- Xu, J., Zhang, J., Liu, J., Yi, K., Xiang, S., Hu, X., Wang, Y., Tao, S., and Ban-Weiss, G.: Influence of cloud microphysical processes on black carbon wet removal, global distributions, and radiative forcing, *Atmos. Chem. Phys.*, 19, 1587-1603, 10.5194/acp-19-1587-2019, 2019.
- [Zhang, Y., Li, M., Cheng, Y., Geng, G., Hong, C., Li, H., Li, X., Tong, D., Wu, N., Zhang, X., Zheng, B., Zheng, Y., Bo, Y., Su, H., and Zhang, Q.: Modeling the aging process of black carbon during atmospheric transport using a new approach: a case study in Beijing, \*Atmos. Chem. Phys.\*, 19, 9663-9680, 10.5194/acp-19-9663-2019, 2019.](#)
- Zheng, B., Tong, D., Li, M., Liu, F., Hong, C., Geng, G., Li, H., Li, X., Peng, L., Qi, J., Yan, L., Zhang, Y., Zhao, H., Zheng, Y., He, K., and Zhang, Q.: Trends in China's anthropogenic emissions since 2010 as the consequence of clean air actions, *Atmos. Chem. Phys.*, 18, 14095-14111, 10.5194/acp-18-14095-2018, 2018.
- [Zhou, X., Gao, J., Wang, T., Wu, W., and Wang, W.: Measurement of black carbon aerosols near two Chinese megacities and the implications for improving emission inventories, \*Atmos. Environ.\*, 43, 3918-3924, <https://doi.org/10.1016/j.atmosenv.2009.04.062>, 2009.](#)
- Zhu, C., Kanaya, Y., Takigawa, M., Ikeda, K., Tanimoto, H., Taketani, F., Miyakawa, T., Kobayashi, H., and Pisso, I.: FLEXPART v10.1 simulation of source contributions to Arctic black carbon, *Atmos. Chem. Phys.*, 20, 1641-1656, 10.5194/acp-20-1641-2020, 2020.
- Zikova, N., and Zdimal, V.: Precipitation scavenging of aerosol particles at a rural site in the Czech Republic, *Tellus B: Chemical and Physical Meteorology*, 68, 27343, 10.3402/tellusb.v68.27343, 2016.

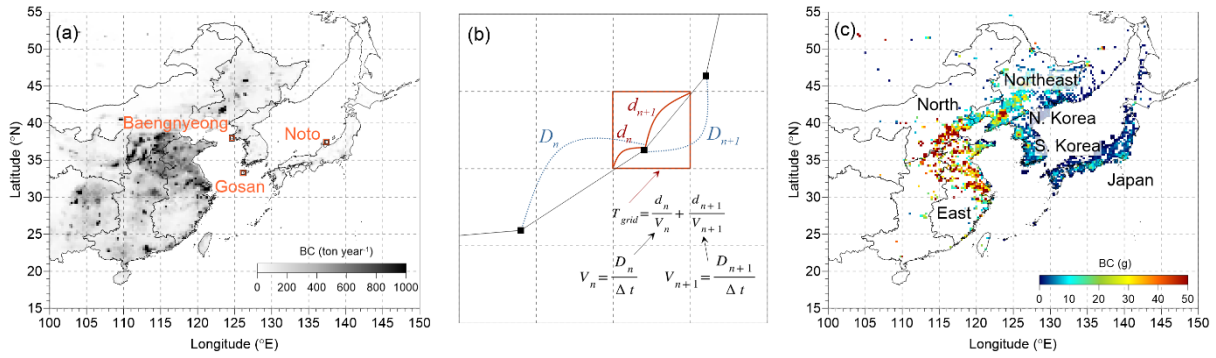


**Figure 1.** (a) The location of three measurement sites (Baengnyeong, Gosan, and Noto) and the black carbon (BC) emission rate ( $\text{ton year}^{-1}$ ) over East Asia from the Regional Emission inventory in ASia (REAS) version 2.1 (Kurokawa et al., 2013). (b) Illustration of residence time calculated based on the HYSPLIT backward trajectory that passed over a single grid cell (see details in the manuscript). (c) The location of administrative districts and The spatial distribution of the mean BC mass in the potential emission region, which is the highest BC mass grid of each trajectory. The BC mass was obtained by multiplying (a) the emission rates and (b) the residence time.

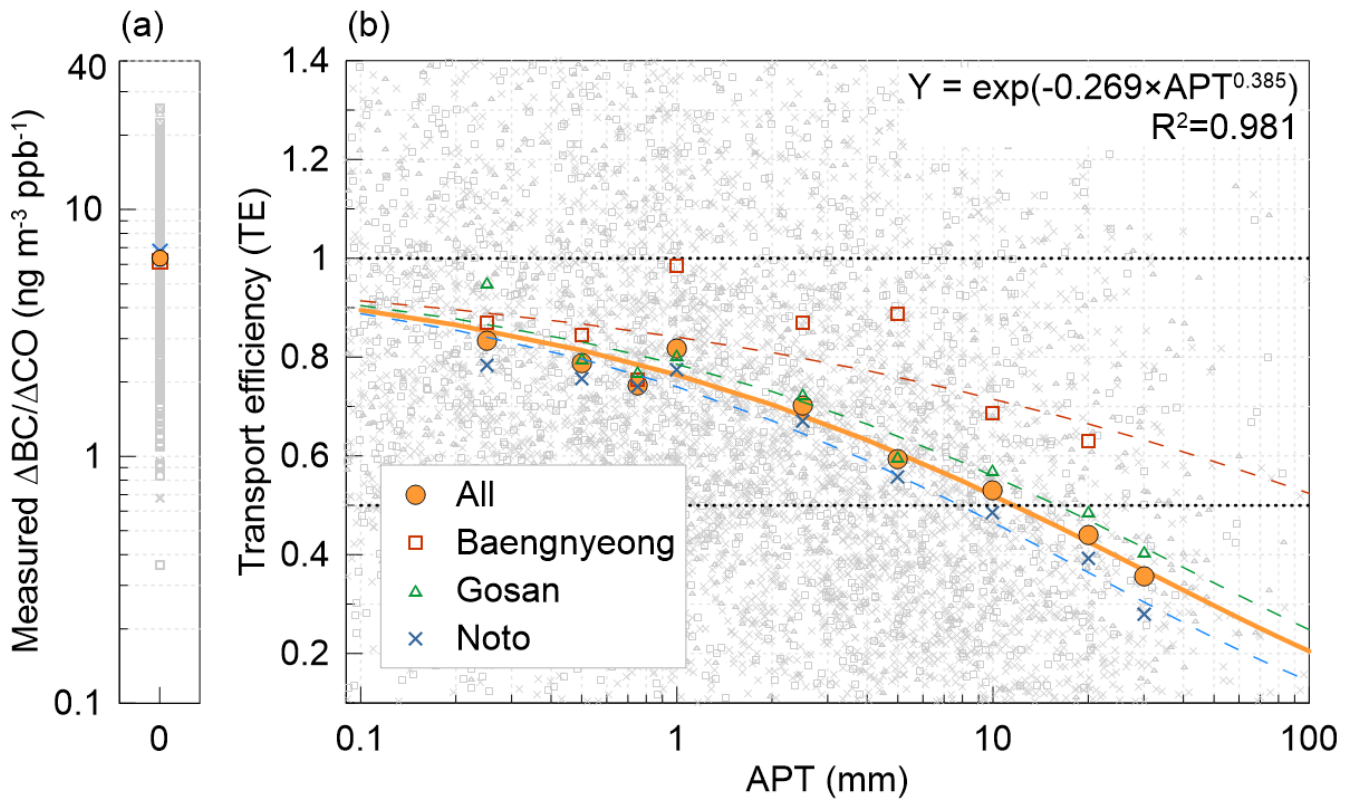


**Figure 2.** Measured  $\Delta BC/\Delta CO$  ratios when accumulated precipitation along trajectory (APT) was zero (left panel) and transport efficiency (TE) variation as a function of APT (right panel) depending on the different sites and overall cases. All data (gray with different symbols) and 9 bins sorted by APT (different colored symbols) are shown. The horizontal dotted lines indicate TE at 0.5 and 1, respectively. The 9 bins consist of 0.01–0.25, 0.25–0.50, 0.50–0.75, 0.75–1.0, 1.0–2.5, 2.5–5.0, 5.0–10, 10–20, and 20–30 mm.

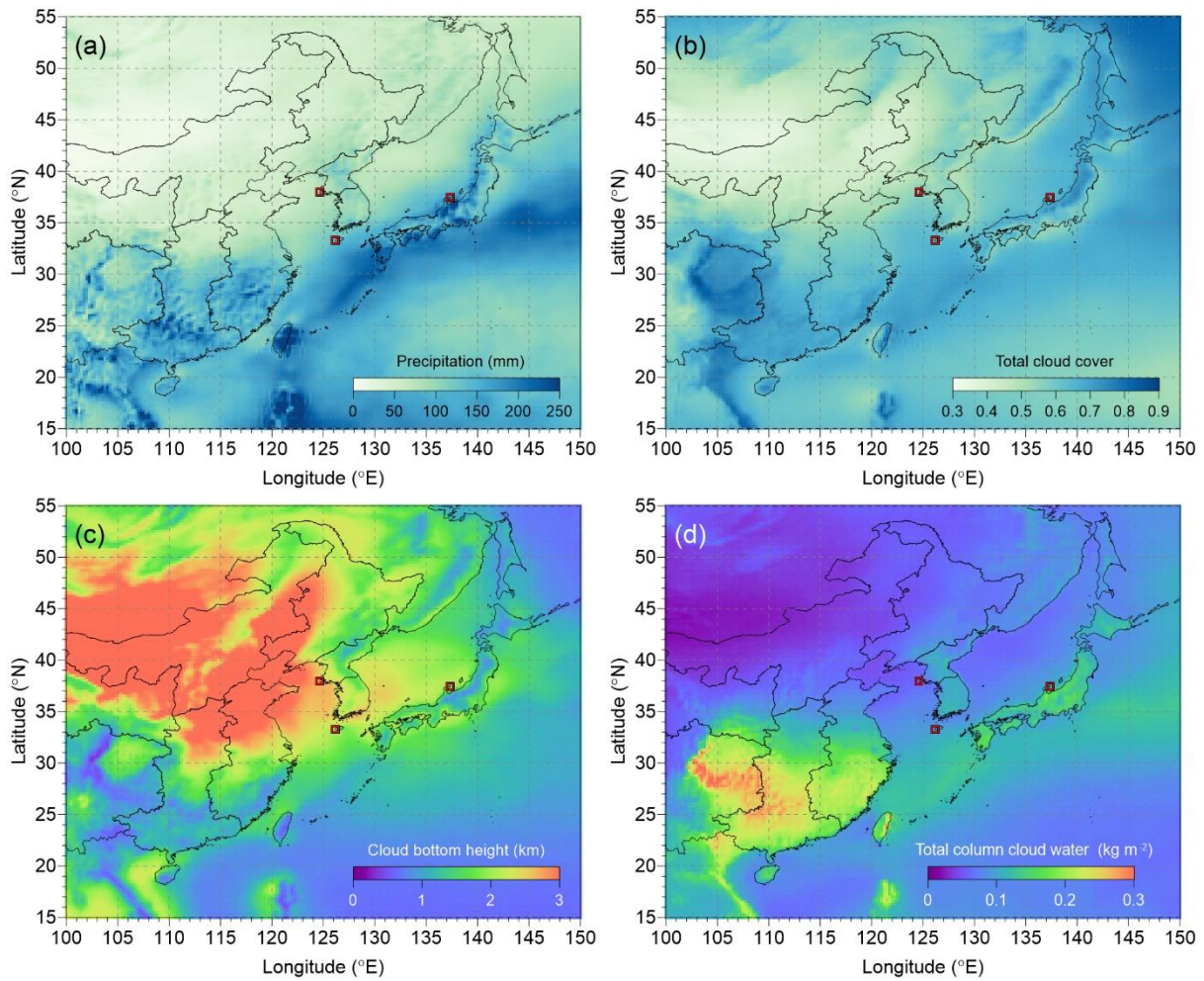


**Figure 3.** Monthly mean meteorological fields over East Asia from 2010 to 2016 derived from the European Centre for Medium-Range Weather Forecasts (ECMWF) ERA5 monthly averaged data at single levels; (a) precipitation (mm), (b) total cloud cover, (c) cloud bottom height (km), and (d) total column cloud total water (ice and liquid).

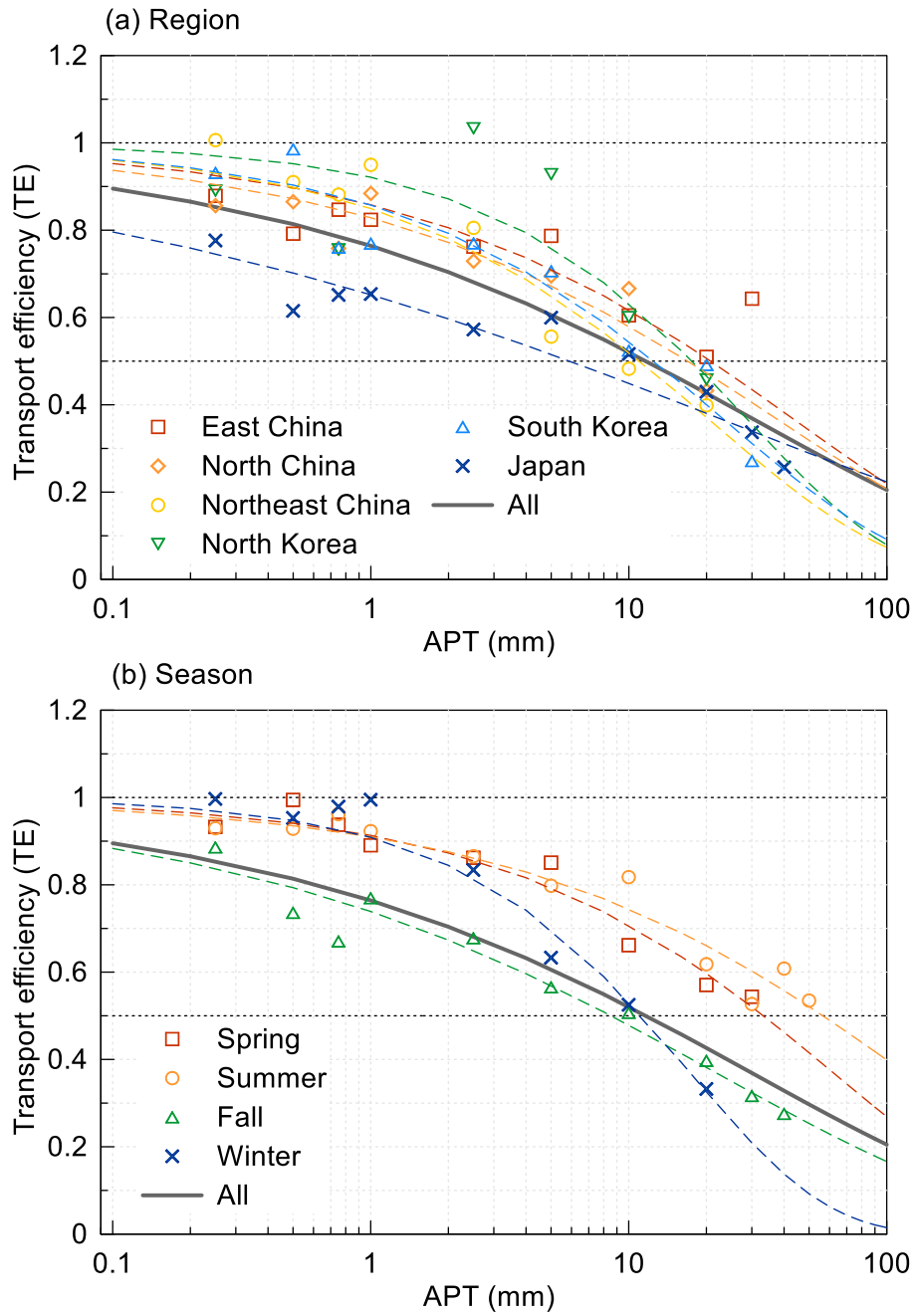


**Figure 4.** Same as Figure 2 except for (a) regional and (b) seasonal variations of TE according to APT. Each colored symbol and dashed line indicate the different regions and seasons and fitting lines according to stretched exponential decay (SED). The thick gray line depicts the overall fitting line. The horizontal dotted lines indicate TE at 0.5 and 1, respectively.



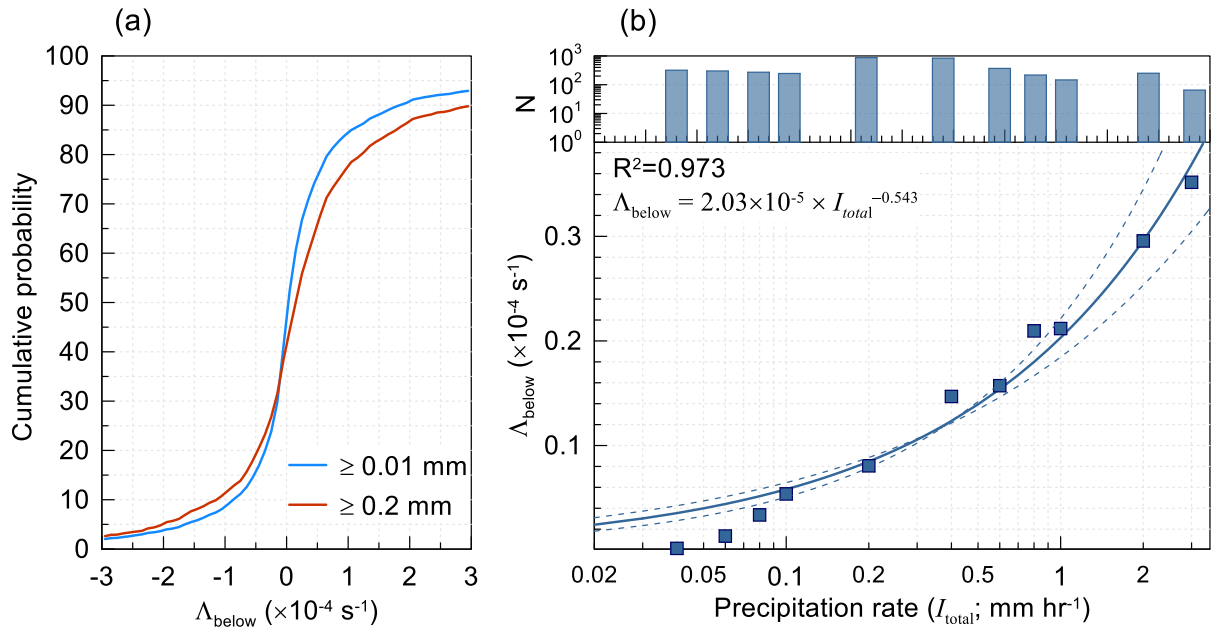


**Figure 5.** (a) Empirical cumulative distribution plot of measured below-cloud scavenging coefficients ( $\Lambda_{\text{below}}$ ;  $\text{s}^{-1}$ ) depending on the precipitation rate ( $\geq 0.01$  and  $\geq 0.2 \text{ mm hr}^{-1}$ ). (b) Median measured  $\Lambda_{\text{below}}$  as a function of the precipitation intensity ( $\text{mm hr}^{-1}$ ) of 11 bins. The dashed line indicates the fit from the equation. The upper panel of (b) shows the number of hourly data points for each bin for  $I_{\text{total}}$ . The 11 bins consist of 0.01–0.04, 0.04–0.06, 0.06–0.08, 0.08–0.1, 0.1–0.2, 0.2–0.4, 0.4–0.6, 0.6–0.8, 0.8–1, 1–2, and 2–3  $\text{mm hr}^{-1}$ .

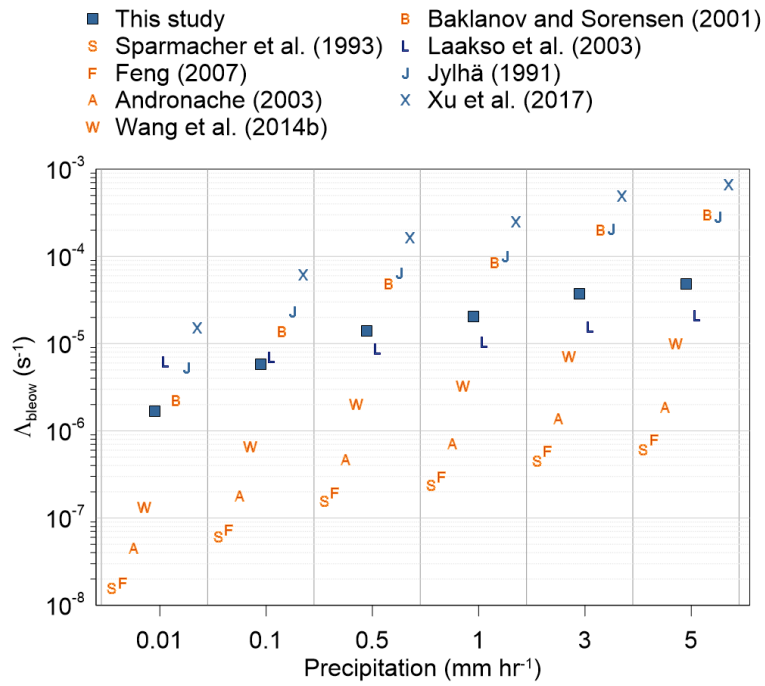


**Figure 6.** Variations in calculated and measured below-cloud scavenging coefficients ( $\Lambda_{\text{below}}$ ; s<sup>-1</sup>) depending on the precipitation intensity (mm hr<sup>-1</sup>). Orange and blue symbols depict the  $\Lambda_{\text{below}}$  equation based on theoretical calculations and observation data, respectively. The diameter of BC was assumed to be approximately 200 nm in the calculation.

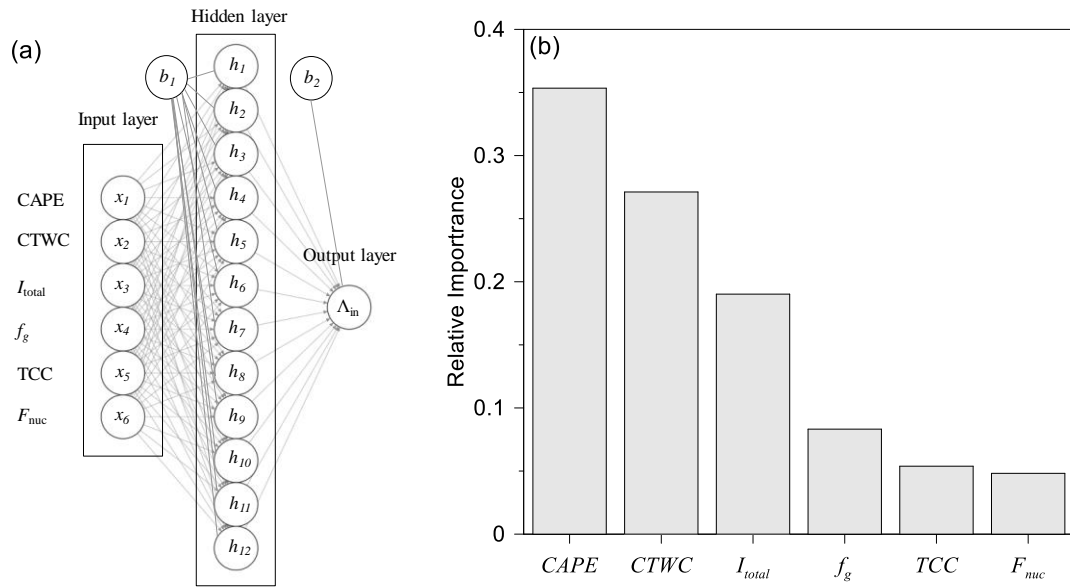


**Figure 7.** (a) Schematic of an artificial neuron network (ANN) model with 12 nodes of a single hidden layer. (b) The relative importance of six input meteorological variables used for calculating in-cloud scavenging coefficients in the FLEXPART model (except for CAPE) using Garson’s algorithm implemented in the ‘NeuralNetTools’ package in R. CAPE, CTWC,  $I_{total}$ ,  $f_g$ , TCC, and  $F_{nuc}$  represent the convective available potential energy, specific cloud total water content, precipitation rate, fraction of a subgrid in a grid cell (see manuscript for details), total cloud cover, and nucleation efficiency, respectively.

**Table 4.** Summary of the relationship between transport efficiency (TE) and accumulated precipitation along trajectory (APT) in Figures 2 and 4.

	Fitting parameters <sup>a</sup>		R <sup>2</sup>	APT (mm)		Number of data points		Days		Annual Precipitation (mm)
	A <sub>1</sub>	A <sub>2</sub>		TE=0.5	TE=1/e	N <sub>APT=0</sub>	N <sub>APT&gt;0</sub> <sup>b</sup>	TE=0.5	TE=1/e	
All	0.269 ± 0.039	0.385 ± 0.035	0.981	11.7	30.2	3,565	6,611	2.8	7.1	1542.3
Site										
Baengnyeong	0.156 ± 0.117	0.350 ± 0.146	0.773	70.9	201.9	1,732	1,522	35.5	101.2	728.3
Gosan	0.235 ± 0.047	0.386 ± 0.047	0.964	16.4	42.3	705	1,090	4.9	12.5	1233.3
Noto	0.306 ± 0.052	0.393 ± 0.036	0.985	8.0	20.3	1,128	4,057	1.1	2.8	2665.3
Region										
East	0.153 ± 0.099	0.498 ± 0.183	0.866	20.7	43.3	439	704			
North	0.188 ± 0.090	0.462 ± 0.175	0.897	16.9	37.3	518	495			
Northeast	0.163 ± 0.084	0.603 ± 0.166	0.945	11.0	20.3	1,237	2,175			
N. Korea	0.082 ± 0.414	0.745 ± 0.813	0.656	17.5	28.7	216	393			
S. Korea	0.154 ± 0.110	0.596 ± 0.188	0.922	12.5	23.2	325	680			
Japan	0.428 ± 0.117	0.272 ± 0.089	0.925	5.9	22.6	687	1,789			
Season										
Spring	0.122 ± 0.045	0.506 ± 0.111	0.957	31.2	64.5	1,285	1,366			
Summer	0.143 ± 0.107	0.362 ± 0.182	0.780	77.3	212.6	497	1,685			
Fall	0.288 ± 0.055	0.397 ± 0.057	0.972	9.1	23.0	767	1,606			
Winter	0.070 ± 0.048	0.905 ± 0.192	0.964	12.5	18.7	1,016	1,986			

<sup>a</sup> TE = exp(-A<sub>1</sub> × APT<sup>A<sub>2</sub></sup>)

<sup>b</sup> The number of satisfactory data points in each bin relative to total N<sub>APT>0</sub> ≥ 2%

**Table 5.** Summaries of the transport efficiency (TE) and scavenging coefficients for selected (a) below- and (b) in-cloud cases based on ERA5 hourly data of pressure levels from ECMWF.

Cases	Median	Interquartile range (25 <sup>th</sup> percentile – 75 <sup>th</sup> percentile)
(a) Below cloud ( $N_{case} = 831$ )		
TE	0.89	[0.61 – 1.27]
<del>Estimated-Measured</del> $\Lambda_{below}$ ( $s^{-1}$ )	$4.01 \times 10^{-6}$	$[2.70 \times 10^{-6} - 6.33 \times 10^{-6}]$
<del>FLEXPART-Calculated</del> $\Lambda_{below}$ ( $s^{-1}$ ) <sup>a</sup>	$6.63 \times 10^{-6}$	$[6.38 \times 10^{-6} - 7.08 \times 10^{-6}]$
(b) In-cloud ( $N_{case} = 769$ )		
TE	0.72	[0.43 – 1.06]
<del>Estimated-Measured</del> $\Lambda_{in}^*$ ( $s^{-1}$ ) <sup>ab</sup>	$8.06 \times 10^{-5}$	-
<del>FLEXPART-Calculated</del> $\Lambda_{in}^*$ ( $s^{-1}$ ) <sup>a, b</sup>	$7.28 \times 10^{-6}$	-

<sup>a)</sup> Calculated using FLEXPART scheme

<sup>ab)</sup> Overall median value

*Supplement of*

**Investigation of the wet removal rate of black carbon in East Asia: validation of a below- and in-cloud wet removal scheme in FLEXPART v10.4**

**Yongjoo Choi et al.**

*Correspondence to:* Yongjoo Choi (choingjoo@jamstec.go.jp)

## **S1 Uncertainty in the transport efficiency (TE) and below- and in-cloud scavenging coefficients**

Our main results, including the TE,  $\Lambda_{\text{below}}$ , and  $\Lambda_{\text{in}}$ , could be influenced by selecting (1) different starting altitudes of the backward trajectories and (2) different altitude criteria for identifying the potential emission region.

First, to investigate the uncertainty caused by different starting altitudes of the backward trajectories, we analyzed the Welch's *t*-test for APT derived from starting altitudes of 500 m and 1000 m. The APT between the two datasets did not show a significant difference (3%) ( $p \geq 0.1$ ). Depending on the site, the TE showed a significant difference ( $p < 0.05$ ) at Gosan only at a relatively small value of  $-4.2\%$ . In the case of regional TE, Northeast China and South Korea were significantly different ( $p < 0.01$ ), with original values up to  $-15\%$ ; however, the corresponding APT for achieving TE=0.5 and TE=1/*e* only decreased by  $-6\%$  and  $-2\%$ , respectively. The regional wet removal efficiency was more apparent, such as more or less APT needed to attain TE=0.5 and TE=1/*e* in low-efficiency regions (East and North China) and high-efficiency regions (South Korea and Japan), respectively. For the high starting altitude, i.e., 1000 m, the air mass had a higher chance of being exposed to in-cloud scavenging resulting in a much lower TE for in-cloud scavenging ( $-3\%$ ). Otherwise, the TE for below-cloud scavenging cases was increased by 7% because of a reduced chance to expose washout effects (Table S1). Because of the variations in the TE for below- and in-cloud scavenging cases, the calculated median  $\Lambda_{\text{below}}$  and  $\Lambda_{\text{in}}$  converged within a similar range as the original results. It should be noted that the median measured  $\Lambda_{\text{below}}$  was slightly higher than the calculated  $\Lambda_{\text{below}}$  according to FLEXPART, which is opposite the original results. The small difference could be ignored when considering the insufficient sample number for below-cloud cases at a starting altitude of 1000 m.

Second, we also checked the difference in wet scavenging efficiency, which can be caused by applying 1.5 km (instead of 2.5 km) as a threshold to determine the potential emission region. The identified six administrative districts for potential emission regions at an altitude of 1.5 km were same as those at an altitude of 2.5 km. The median traveling time from potential source regions to receptor sites was decreased from 38 h to 25 h when precipitation occurred because the individual potential source region was closer to the receptor site because the selection altitude was decreased. However, the difference in traveling time did not significantly influence our final results because the TE for below- and in-cloud cases only decreased by 1% and 6% and the measured  $\Lambda_{\text{below}}$  and  $\Lambda_{\text{in}}$  were consistent with the original results within  $\pm 54\%$  (Table S2). From these results, we confirmed the representativeness of our regional and seasonal wet removal efficiency analysis.

## **S2 Difference in air mass pathways and accumulated precipitation along trajectory (APT) between HYSPLIT and FLEXPART**

We investigated the uncertainty in the air mass pathway and APT between HYSPLIT model using ERA5 and FLEXPART using ERA-Interim during study periods at three sites. It should be noted that the trajectory of FLEXPART was selected as the center of the main grid ( $1^\circ \times 1^\circ$ ) according to the highest residence time in the same time interval and then compared with HYSPLIT results by calculating the distance between two hourly endpoints. Thus, differences of less than  $\sim 100$  km can be regarded as a good agreement when considering the grid resolution of FLEXPART. The difference in distance increased as the traveling time was increased. However, the median traveling time of air masses, including APT=0 case, was 31 h, which showed a difference in distance of  $\sim 100$  km. When the traveling time was expanded up to the 75%ile of the traveling time (50 h), the difference in distance was close to  $\sim 200$  km. Although the difference in distance at 72 h traveling time was high, 72 h traveling time cases was so rare that we could neglect the impacts on our results. In total, the median difference in distance was  $\sim 47$  km, suggesting good agreement between the two datasets. In addition, the difference in accumulated backward-trajectory endpoints

was much smaller because random errors in the single calculations can be diminished by increasing the number of calculations (Gebhart et al., 2005; Jeong et al., 2017).

Figure S2 presents the cumulative probability of APT from HYSPLIT and FLEXPART. Although the air mass pathway showed insignificant differences between the two models, the median APT of FLEXPART (1.2 mm) was two times higher than that of HYSPLIT (0.63 mm), indicating a higher bias of the FLEXPART APT. This result can be caused by the difference in meteorological input data and the treatment of precipitation fields, homogeneous precipitation in a single grid cell ( $0.25^{\circ} \times 0.25^{\circ}$ ) in HYSPLIT and disaggregated precipitation induced by interpolating in time and space in FLEXPART (Hittmeir et al., 2018). The higher bias in the FLEXPART APT contributed to increasing the magnitude of the underestimation of FLEXPART TE when assuming the same APT from HYSPLIT model, indicating an insignificant impact on the results.

Gebhart, K.A., Schichtel, B.A., Barna, M.G.: Directional biases in back trajectories caused by model and input data. *J. Air Waste Manag.* 55, 1649-1662, 2005.

Jeong, U., Kim, J., Lee, H., Lee, Y.G.: Assessing the effect of long-range pollutant transportation on air quality in Seoul using the conditional potential source contribution function method. *Atmos. Environ.*, 150, 33-44, 2017.

Hittmeir, S., Philipp, A., and Seibert, P.: A conservative reconstruction scheme for the interpolation of extensive quantities in the Lagrangian particle dispersion model FLEXPART. *Geosci. Model Dev.*, 11, 2503-2523, <https://doi.org/10.5194/gmd-11-2503-2018>, 2018.



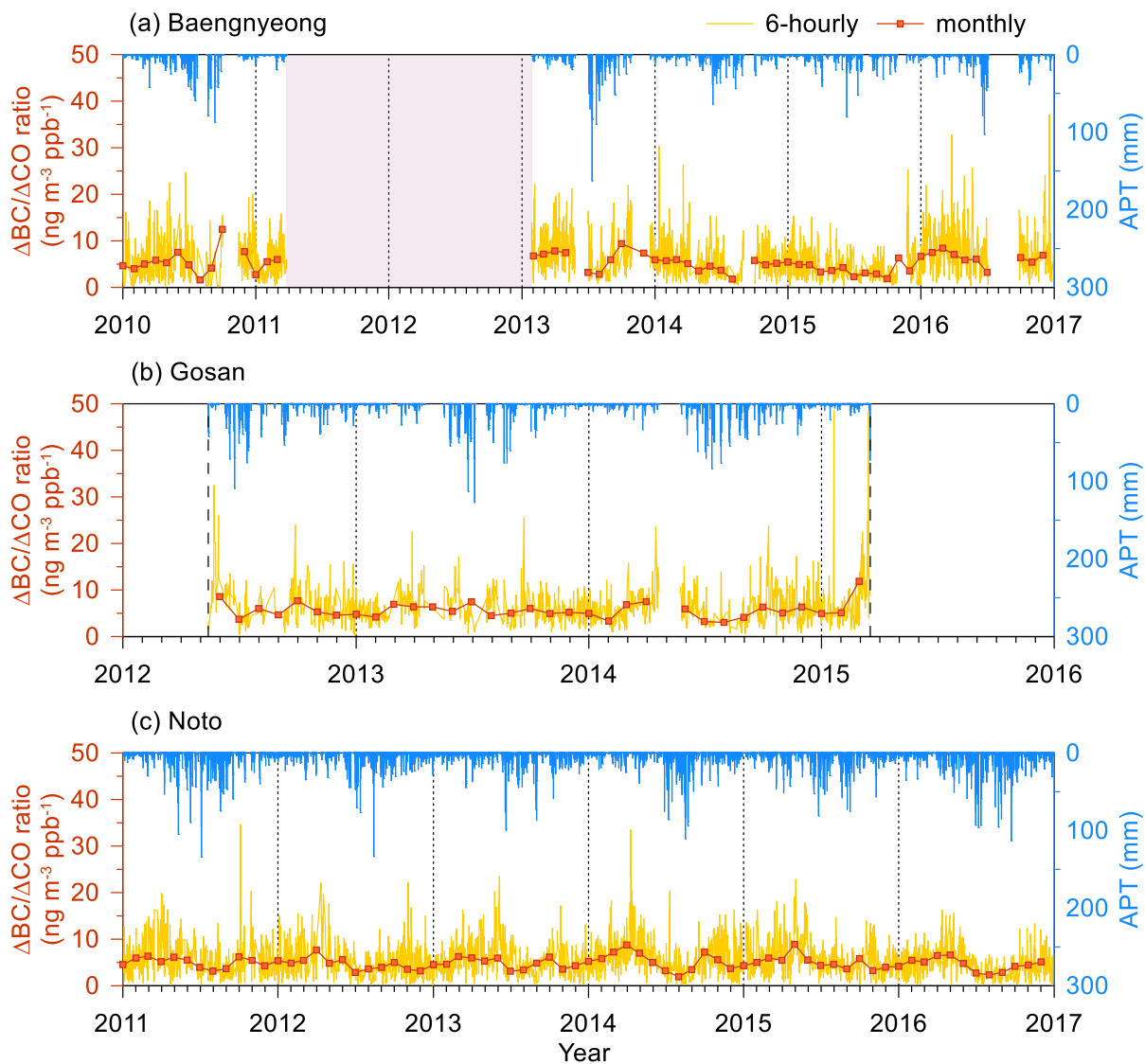


**Figure S1.** Time series of the  $\Delta BC/\Delta CO$  ratio and accumulated precipitation along trajectory (APT) during the measurement periods in (a) Baengnyeong (1 Jan 2010–31 Dec 2016), (b) Gosan (1 May 2012–30 Apr 2015), and (c) Noto (1 Jan 2011–31 Dec 2016). The square symbols with solid lines indicate monthly concentrations. The red shaded region in the Baengnyeong figure indicates periods of data missing from 2011 to 2012 due to the absence of CO data.

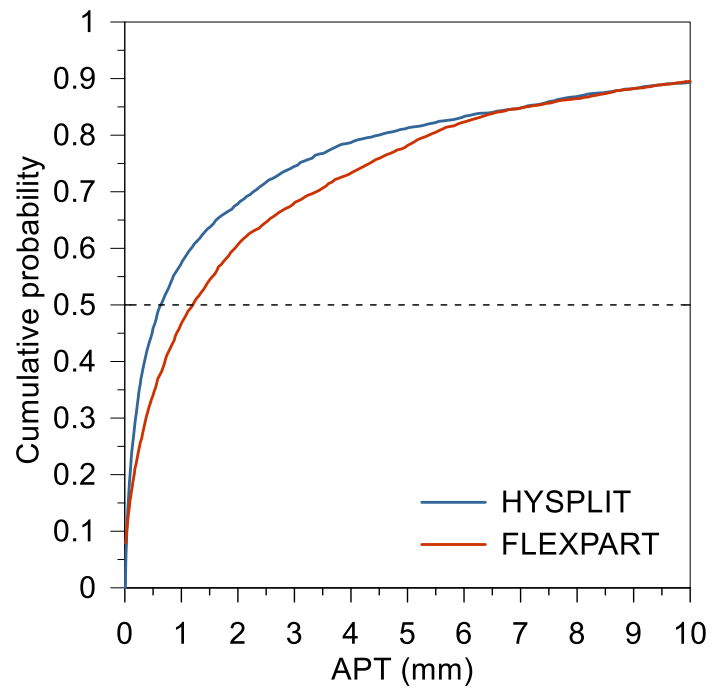


**Figure S2.** Cumulative probability plot of the APT from HYSPLIT (blue) and FLEXPART (red) during the study periods at the three sites. The dashed black line indicated a cumulative probability at 0.5 (median).

**Table S1.** Same as Table 2 except for the different backward trajectory starting altitudes (1000 m)

Cases	Median	Interquartile range (25 <sup>th</sup> percentile – 75 <sup>th</sup> percentile)
(a) Below cloud ( $N_{case} = 262$ )		
TE	0.95	[0.65 – 1.28]
Measured $\Lambda_{below}$ ( $s^{-1}$ )	$8.85 \times 10^{-6}$	$[6.57 \times 10^{-6} - 1.46 \times 10^{-5}]$
Calculated $\Lambda_{below}$ ( $s^{-1}$ ) <sup>a</sup>	$7.49 \times 10^{-6}$	$[6.83 \times 10^{-6} - 8.42 \times 10^{-6}]$
(b) In-cloud ( $N_{case} = 953$ )		
TE	0.70	[0.46 – 1.02]
Measured $\Lambda_{in}^*$ ( $s^{-1}$ ) <sup>b</sup>	$7.67 \times 10^{-5}$	-
Calculated $\Lambda_{in}^*$ ( $s^{-1}$ ) <sup>a,b</sup>	$8.01 \times 10^{-6}$	-

a) Calculated using FLEXPART scheme  
b) Overall median value

**Table S2.** Same as Table 2 except for the different altitude criteria (1.5 km) for identifying potential emission source regions.

Cases	Median	Interquartile range (25 <sup>th</sup> percentile – 75 <sup>th</sup> percentile)
(a) Below cloud ( $N_{case} = 436$ )		
TE	0.88	[0.60 – 1.24]
Measured $\Lambda_{below}$ ( $s^{-1}$ )	$6.17 \times 10^{-6}$	$[2.55 \times 10^{-6} - 1.39 \times 10^{-5}]$
Calculated $\Lambda_{below}$ ( $s^{-1}$ ) <sup>a</sup>	$7.52 \times 10^{-6}$	$[6.88 \times 10^{-6} - 8.50 \times 10^{-6}]$
(b) In-cloud ( $N_{case} = 282$ )		
TE	0.68	[0.44 – 1.03]
Measured $\Lambda_{in}^*$ ( $s^{-1}$ ) <sup>b</sup>	$9.39 \times 10^{-5}$	-
Calculated $\Lambda_{in}^*$ ( $s^{-1}$ ) <sup>a,b</sup>	$8.15 \times 10^{-6}$	-

a) Calculated using FLEXPART scheme  
b) Overall median value